2017

Tropospheric emissions: Monitoring of pollution (TEMPO)

P. Zoogman
Harvard-Smithsonian Center for Astrophysics

X. Liu
Harvard-Smithsonian Center for Astrophysics

R. M. Suleiman
Harvard-Smithsonian Center for Astrophysics

W. F. Pennington
NASA Langley Research Center

D. E. Flittner
NASA Langley Research Center

See next page for additional authors

Authors
P. Zoogman, X. Liu, R. M. Suleiman, W. F. Pennington, D. E. Flittner, J. A. Al-Saadi, B. B. Hinton, D. K. Nicks, M. J. Newchurch, J. L. Carr, S. J. Janz, M. R. Andraschko, A. Arola, B. D. Baker, B. P. Canova, C. Chan Miller, R. C. Cohen, J. E. Davis, M. E. Dussault, D. P. Edwards, J. Fishman, A. Ghulam, G. Gonzalez Abad, M. Grutter, J. R. Herman, J. Houck, D. J. Jacob, J. Joiner, B. J. Kerridge, J. Kim, N. A. Krotkov, L. Lamsal, C. Li, A. Lindfors, R. V. Martin, C. T. McElroy, C. McLinden, V. Natraj, D. O. Neil, C. R. Nowlan, E. J. O'Sullivan, P. I. Palmer, R. B. Pierce, M. R. Pippin, A. Saiz-Lopez, R. J. D. Spurr, J. J. Szykman, O. Torres, J. P. Veefkind, B. Veihelmann, H. Wang, and J. Wang

Journal of Quantitative Spectroscopy & Radiative Transfer 186 (2017) 17–39

Contents lists available at ScienceDirect

Journal of Quantitative Spectroscopy & Radiative Transfer

journal homepage: www.elsevier.com/locate/jqsrt

Tropospheric emissions: Monitoring of pollution (TEMPO)

P. Zoogman [a,*], X. Liu [a], R.M. Suleiman [a], W.F. Pennington [b], D.E. Flittner [b], J.A. Al-Saadi [b], B.B. Hilton [b], D.K. Nicks [c], M.J. Newchurch [d], J.L. Carr [e], S.J. Janz [f], M.R. Andraschko [b], A. Arola [g], B.D. Baker [c], B.P. Canova [c], C. Chan Miller [h], R.C. Cohen [i], J.E. Davis [a], M.E. Dussault [a], D.P. Edwards [j], J. Fishman [k], A. Ghulam [k], G. González Abad [a], M. Grutter [l], J.R. Herman [m], J. Houck [a], D.J. Jacob [h], J. Joiner [f], B.J. Kerridge [n], J. Kim [o], N.A. Krotkov [f], L. Lamsal [f,p], C. Li [f,m], A. Lindfors [g], R.V. Martin [a,q], C.T. McElroy [r], C. McLinden [s], V. Natraj [t], D.O. Neil [b], C.R. Nowlan [a], E.J. O'Sullivan [a], P.I. Palmer [u], R.B. Pierce [v], M.R. Pippin [b], A. Saiz-Lopez [w], R.J.D. Spurr [x], J.J. Szykman [y], O. Torres [f], J.P. Veefkind [z], B. Veihelmann [aa], H. Wang [a], J. Wang [ab], K. Chance [a]

[a] *Harvard-Smithsonian Center for Astrophysics, USA*
[b] *NASA Langley Research Center, USA*
[c] *Ball Aerospace & Technologies Corp, USA*
[d] *University of Alabama at Huntsville, USA*
[e] *Carr Astronautics, USA*
[f] *NASA Goddard Space Flight Center, USA*
[g] *Finnish Meteorological Institute, Finland*
[h] *Harvard University, USA*
[i] *University of California at Berkeley, USA*
[j] *National Center for Atmospheric Research, USA*
[k] *Saint Louis University, USA*
[l] *Universidad Nacional Autónoma de México, Mexico*
[m] *University of Maryland, Baltimore County, USA*
[n] *Rutherford Appleton Laboratory, UK*
[o] *Yonsei University, South Korea*
[p] *GESTAR, University Space Research Association, USA*
[q] *Dalhousie University, Canada*
[r] *York University, Canada*
[s] *Environment and Climate Change Canada*
[t] *NASA Jet Propulsion Laboratory, USA*
[u] *University of Edinburgh, UK*
[v] *National Oceanic and Atmospheric Administration, USA*
[w] *Instituto de Química Física Rocasolano, CSIC, Spain*
[x] *RT Solutions, Inc., USA*
[y] *Environmental Protection Agency, USA*
[z] *Koninklijk Nederlands Meteorologisch Instituut, Netherlands*
[aa] *European Space Agency, France*
[ab] *University of Nebraska, USA*

ARTICLE INFO

Article history:
Received 14 February 2016

ABSTRACT

TEMPO was selected in 2012 by NASA as the first Earth Venture Instrument, for launch between 2018 and 2021. It will measure atmospheric pollution for greater North America

* Corresponding author.

http://dx.doi.org/10.1016/j.jqsrt.2016.05.008

Received in revised form
11 May 2016
Accepted 11 May 2016
Available online 6 June 2016

from space using ultraviolet and visible spectroscopy. TEMPO observes from Mexico City, Cuba, and the Bahamas to the Canadian oil sands, and from the Atlantic to the Pacific, hourly and at high spatial resolution ($\sim$2.1 km N/S $\times$ 4.4 km E/W at 36.5°N, 100°W). TEMPO provides a tropospheric measurement suite that includes the key elements of tropospheric air pollution chemistry, as well as contributing to carbon cycle knowledge. Measurements are made hourly from geostationary (GEO) orbit, to capture the high variability present in the diurnal cycle of emissions and chemistry that are unobservable from current low-Earth orbit (LEO) satellites that measure once per day. The small product spatial footprint resolves pollution sources at sub-urban scale. Together, this temporal and spatial resolution improves emission inventories, monitors population exposure, and enables effective emission-control strategies.

TEMPO takes advantage of a commercial GEO host spacecraft to provide a modest cost mission that measures the spectra required to retrieve ozone (O_3), nitrogen dioxide (NO_2), sulfur dioxide (SO_2), formaldehyde (H_2CO), glyoxal ($C_2H_2O_2$), bromine monoxide (BrO), IO (iodine monoxide), water vapor, aerosols, cloud parameters, ultraviolet radiation, and foliage properties. TEMPO thus measures the major elements, directly or by proxy, in the tropospheric O_3 chemistry cycle. Multi-spectral observations provide sensitivity to O_3 in the lowermost troposphere, substantially reducing uncertainty in air quality predictions. TEMPO quantifies and tracks the evolution of aerosol loading. It provides these near-real-time air quality products that will be made publicly available. TEMPO will launch at a prime time to be the North American component of the global geostationary constellation of pollution monitoring together with the European Sentinel-4 (S4) and Korean Geostationary Environment Monitoring Spectrometer (GEMS) instruments.

Contents

1. Introduction

Over the past decades, observation of the atmospheric species from space has become an increasingly powerful tool for understanding the processes that govern atmospheric composition and air quality. However, while past and present satellite measurements provide global coverage, their coarse spatial and temporal sampling preclude

answering many of the current questions relevant to air quality concerning emissions, variability, and episodic events. Conversely, the *in situ* measurements from surface sites that are currently used for air quality monitoring have limited spatial density and coverage. The Tropospheric Emissions: Monitoring of Pollution (TEMPO) geostationary (GEO) mission is planned to address many of the shortcomings of the current atmospheric composition observing system.

The TEMPO instrument will be delivered in 2017 for integration onto the nadir deck of a NASA-selected GEO host spacecraft for launch as early as 2018. TEMPO and its Asian (GEMS) and European (Sentinel-4) constellation partners make the first tropospheric trace gas measurements from GEO, building on the heritage of six spectrometers flown in low-Earth orbit (LEO). These LEO instruments measure the needed spectra, although at coarser spatial and temporal resolutions, to the precisions required for TEMPO. They use retrieval algorithms developed for them by TEMPO Science Team members and that are currently running in operational environments. This makes TEMPO an innovative use of a well-proven technique, able to produce a revolutionary data set.

The 2007 National Research Council (NRC) Decadal Survey "Earth Science and Applications from Space" included the recommendation for the Geostationary Coastal and Air Pollution Events (GEO-CAPE) mission to launch in 2013–2016 to advance the science of both coastal ocean biophysics and atmospheric-pollution chemistry [78]. While GEO-CAPE is not planned for implementation this decade, TEMPO will provide much of the atmospheric measurement capability recommended for GEO-CAPE. Instruments from Europe (Sentinel 4) and Asia (GEMS) will form parts of a global GEO constellation for pollution monitoring within several years, with a major focus on intercontinental pollution transport. Concurrent LEO instruments will observe pollution over oceans [125], which will then be observed by these GEO instruments once they enter each field of regard [130]. TEMPO will launch at a prime time to be a component of this constellation, and is also a pathfinder for the hosted payload mission strategy.

Section 2 outlines the TEMPO mission and provides the historical and scientific background for the mission. Section 3 describes the instrument specifications, design, and expected performance. Sections 4 and 5 give a brief overview of TEMPO implementation and operations, respectively. Section 6 describes TEMPO in the context of a global GEO constellation and international partnerships in North America. Section 7 outlines the trace gas, aerosol, and other science products TEMPO produces along with detailing the state-of-the-science ozone profile retrievals TEMPO performs. Section 8 describes the validation efforts that are part of the TEMPO mission. Section 9 details the various science studies that are enabled by TEMPO. Section 10 outlines the public outreach and education opportunities that we are pursuing related to TEMPO.

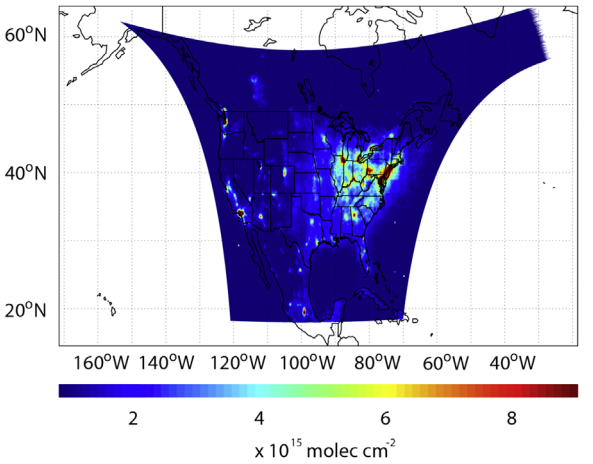

Fig. 1. Average tropospheric column NO_2 for 2005–2008 measured from the OMI satellite over the TEMPO field of regard.

2. TEMPO overview and background

TEMPO collects the space-based measurements needed to quantify variations in the temporal and spatial emissions of gases and aerosols important for air quality with the precision, resolution, and coverage needed to improve our understanding of pollutant sources and sinks on suburban, local, and regional scales and the processes controlling their variability over diurnal and seasonal cycles. TEMPO data products include atmospheric ozone profile, total column ozone, NO_2, SO_2, H_2CO, $C_2H_2O_2$, H_2O, BrO, IO, aerosol properties, cloud parameters, UVB radiation, and foliage properties over greater North America.

Fig. 1 shows the average tropospheric column NO_2 for 2005–2008 measured from the OMI satellite over the TEMPO field of regard. Every hour during daylight, TEMPO will scan this entire greater North American domain that extends from Mexico City to the Canadian oil sands and from the Atlantic to the Pacific. Fig. 2 shows the TEMPO footprint size over the Baltimore-Washington metropolitan area. Together, unprecedented spatial and temporal resolution of TEMPO measurements represents a transformative development in observing the chemical composition of the atmosphere from space.

TEMPO evolved from the GEO-CAPE mission as a concept to achieve as much of the recommended GEO-CAPE atmosphere ultraviolet and visible (UV/Vis) measurement capability as possible within the cost constraints of the NASA Earth Venture Program. To inform design of the GEO-CAPE mission, [130] conducted an observation system simulation experiment (OSSE) to determine the instrument requirements for geostationary satellite observations of ozone air quality in the US. Instruments using different spectral combinations of UV, Vis, and thermal IR (TIR) were analyzed. The GEO-CAPE Simulation Team produced ozone profile retrievals in different spectral combinations [79]. Hourly observations of ozone from geostationary orbit were found to improve the assimilation considerably relative to daily observation from LEO, emphasizing the importance of a geostationary atmospheric composition satellite. UV/Vis, UV/TIR, and UV/Vis/

TIR spectral combinations all improved greatly the information on surface ozone relative to UV alone. Demonstration of the utility of a UV/Vis instrument helped support TEMPO instrument design.

Under support from the GEO-CAPE Mission Preformulation Atmospheric Science Working Group, regional and urban OSSEs are extending this previous GEO-CAPE OSSE. We are conducting high resolution (12 km and 1 km) Community Multiscale Air Quality (CMAQ) model [11] nature runs, utilizing observed surface reflectivity and emissivity to generate synthetic radiances, and including estimates of realistic averaging kernels for each TEMPO retrieval. The ongoing OSSEs utilize diurnally resolved high spectral resolution UV/Vis/thermal-infrared (UV/VIS/TIR) radiative transfer modeling at 14 representative sites using ozone, NO_2, H_2CO, SO_2, aerosol, water vapor, and temperature profiles from the nature run [79]. The OSSE data assimilation studies use the Weather Research and Forecasting with Chemistry (WRF-CHEM) forecast model [34] and the Real-time Air Quality Modeling System (RAQMS) [86]. Preliminary results of these OSSE studies show significant positive impacts of assimilating geostationary ozone retrievals for constraining near-surface ozone compared to assimilating existing polar orbiting instruments.

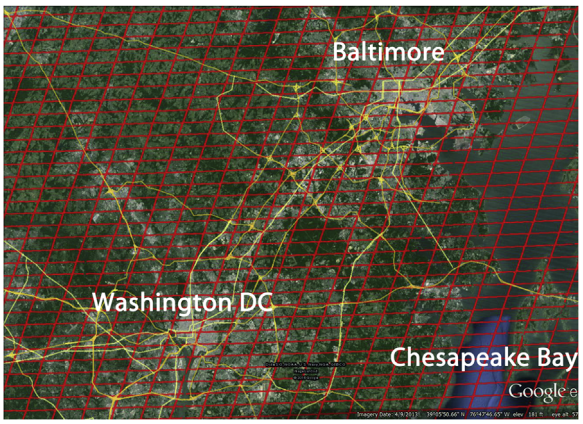

Fig. 2. TEMPO footprints overlaid on the Baltimore-Washington metropolitan area. The footprint size here is approximately 2.5 km N/S × 5 km E/W. Map created using Google Earth/Landsat Imagery.

3. Instrument design and performance

TEMPO is being built at Ball Aerospace & Technologies Corporation (BATC). The TEMPO design addresses important challenges in (1) signal-to-noise using high system throughput, cooled detectors and on-board co-additions of images; (2) thermal management using design and cold biasing with active heater control (3) Image Navigation and Registration (INR) using closed-loop scan mirror control and ground processing using tie-points into well navigated GOES imagery. The instrument Critical Design Review was completed in June 2015. Table 1 lists expected performance values for key instrument parameters for a geostationary spacecraft at 100°W.

TEMPO will be integrated to the host spacecraft with the nominal optical axis pointed at 36.5°N, 100°W (~5.8° from spacecraft nadir). Its field of regard is designed to cover greater North America as seen from any GEO orbit longitude within 80°W to 115°W. The TEMPO instrument consists of a number of subsystems as indicated in the block diagram shown in Fig. 3. The yellow arrows indicate the path of light from the aperture through the optical assembly to the focal plane subsystem. Each subsystem is described below.

Table 1.
Key TEMPO instrument parameters based on the latest design as of February 2016 for a geostationary satellite at 100°W. The signal to noise ratio is the average value over the specific retrieval windows for the nominal radiance spectrum. IFOV is Instantaneous Field of View at 36.5°N, 100°W. MTF is Modulation Transfer Function at Nyquist.

Parameter		Value	Parameter	Value
Mass		148 kg	Spectral range	290–490 nm, 540–740 nm
Volume		1.4 × 1.1 × 1.2 m	Spectral resolution & sampling	0.57 nm, 0.2 nm
Avg. operational power		163 W	Albedo calibration uncertainty	2.0% λ-independent, 0.8% λ-dependent
Average Signal to Noise [hourly @ 8.4 km x 4.4 km]	O_3:Vis (540–650 nm)	1436	Spectral uncertainty	< 0.1 nm
	O_3: UV (300–345 nm)	1610	Polarization factor	≤ 2% UV, < 10% Vis
	NO_2: 423–451 nm	1771	Revisit time	1 h
	H_2CO: 327–356 nm	2503	Field of regard: N/ S × E/W	4.82° × 8.38° (greater North America)
	SO_2: 305–345 nm	1797	Geo-location Uncertainty	2.8 km
	$C_2H_2O_2$: 420–480 nm	1679	IFOV: N/S × E/W	2.1 km × 4.4 km
	Aerosol: 354, 388 nm	2313	E/W oversampling	5%
	Clouds: 346–354 nm	2492	MTF of IFOV: N/S × E/W	0.19 × 0.36

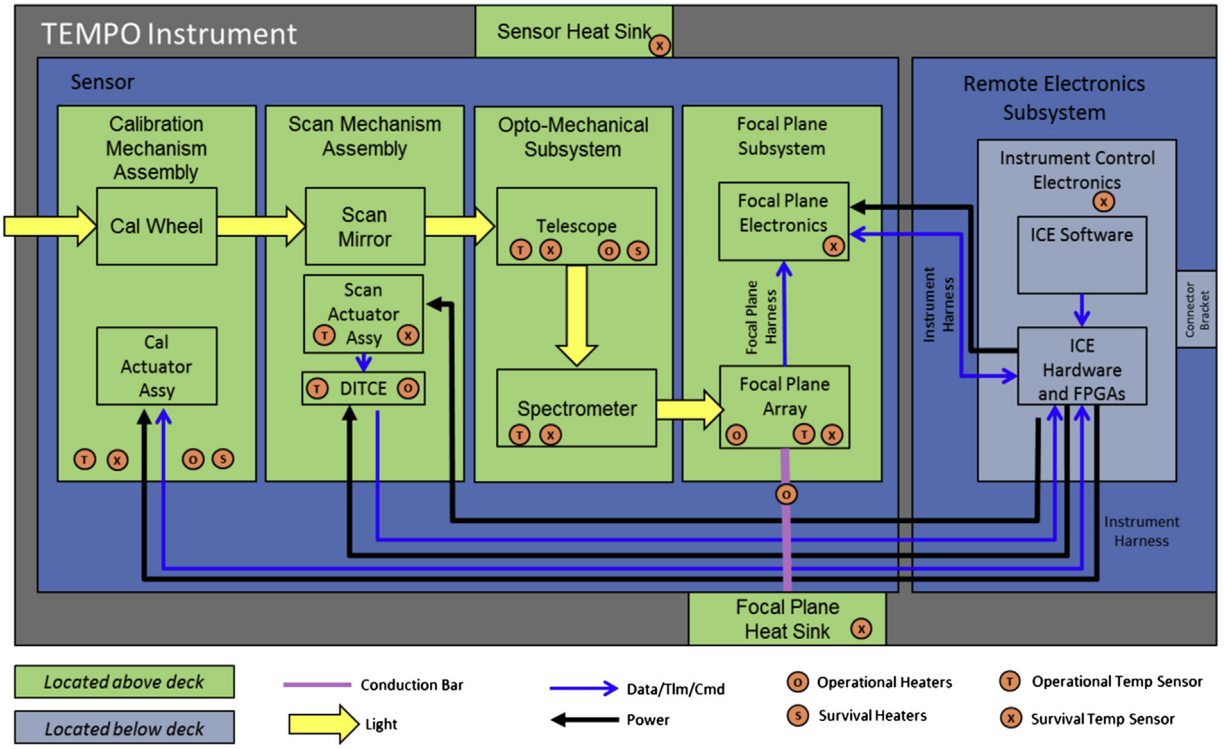

Fig. 3. TEMPO instrument functional block diagram. FPGAs – Field-Programmable Gate Arrays. DITCE – Differential Impedance Transducer Conditioning Electronics.

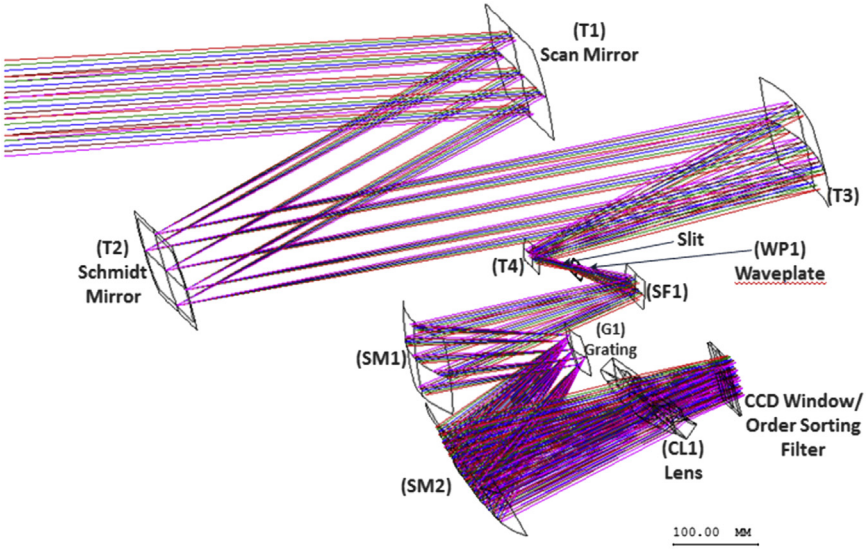

Fig. 4. Optical ray trace for the TEMPO instrument, including telescope and spectrometer.

The Calibration Mechanism Assembly (CMA) controls the instrument aperture. It consists of a wheel containing four selectable positions: Closed, open, working diffuser and reference diffuser. The ground fused silica diffusers allow recording of the top-of-atmosphere solar irradiance. Earth-view radiance measurements are made in the open position. The working diffuser is used on a daily basis and the reference diffuser is used to trend any degradation of the working diffuser from radiation exposure and contamination. Dark scene data are collected with the wheel in the closed position.

The Scan Mechanism Assembly (SMA) steps the projected TEMPO instrument slit image, or field of view (FOV, aligned in the North-South direction) across the TEMPO

field of regard and compensates for unwanted spacecraft motion [95]. When the instrument is collecting image data, the FOV is held stable at a given ground location while individual images are recorded before stepping to the next location. The SMA is housed as the first optic within the telescope optical assembly. The SMA consists of a silicon carbide mirror gimbaled to a two-axis mechanism involving two flex pivots per axis. The mechanism is actuated inductively using a network of voice coils and magnets. The mirror position is measured using differential impedance transducers (DITs). The SMA is close-loop controlled using real-time attitude data supplied by the host spacecraft.

The Opto-Mechanical Subsystems consist of a telescope and a spectrometer assembly. Primarily, the optical design employs reflective optics with simple geometries (Fig. 4). The *f*/3 Schmidt-form telescope consists of the T1 Scan mirror, the T2 Schmidt mirror and a T3 and T4 with final projection onto the slit of the spectrometer assembly. The telescope mirrors are coated with UV-enhanced aluminum, with the exception of the T2 optic, which has a band-blocking coating to minimize stray light biases within the spectrometer.

The Offner-type spectrometer was chosen due to its compact design and superior re-imaging performance and is similar to the Ozone Mapping Profiler Suite (OMPS) nadir spectrometer [24]. The spectrometer consists of a slit, a quartz wave plate (for polarization mitigation), a diffraction grating, a corrector lens and a CCD window/order sorting filter. The mechanically ruled grating (500 lines/mm) is a convex paneled (3 partite) optic with a blaze angle of 5° at 325 nm. The optical benches are a truss-type design constructed of composite tubes with titanium fittings. The Opto-mechanical system is athermal and actively temperature-controlled for superior spectral stability over changing diurnal and seasonal thermal environments.

The Focal Plane Array (FPA) and Focal Plane Electronics (FPE) comprise the focal plane subsystem. The FPA contains two separate, but identically designed, $1\,K \times 2\,K$ pixels, full-frame transfer, charge coupled device (CCD) detectors. There are 2 K pixels each in the spatial direction (along the slit) and 1 K pixels each in the spectral direction. 290 nm to 490 nm is measured by the UV CCD and 540 nm to 740 nm by the Vis CCD. The CCDs are back-thinned and have an anti-reflection coating for enhanced operation in the UV. The CCDs are read-out and digitized simultaneously to create spectra with the same period of integration ($\sim$118 ms in duration). Multiple integrations ($\sim$21) are added together on-board, for a single scan mirror position, before transferring to the host spacecraft for downlink. The CCDs are passively cooled with a dedicated thermal connection to a cold biased spacecraft thermal interface and stabilized with a heater on the thermal connection. The spectral regions to be measured by TEMPO are illustrated in Fig. 5 by reflectances for various scenes measured by the European Space Agency's GOME-1 instrument.

The TEMPO INR solution uses a combination of flight hardware and ground software, as shown in Fig. 6, to accurately assign geographic locations to pixels and assure uniform, gapless, and efficient coverage of greater North America. TEMPO INR relies on GOES weather satellite imagery for pointing truth [13]. This is available with ≤ 5 min latency with respect to real time and is more accurately registered to the Earth than that required by TEMPO. First, a GOES-like image is constructed by weighting the TEMPO spectral planes in accordance with the GOES relative spectral response function. Next, templates are extracted from the GOES-like image and matched against GOES imagery, creating a set of tie-point measurements in progression as TEMPO scans across the domain.

A Kalman filter with a high-fidelity model of the TEMPO system embedded within it is at the heart of the TEMPO INR system. Its state vector is updated with each tie-point measurement and propagated in between measurements using modeled dynamics and spacecraft attitude telemetry from onboard gyroscopes. A tracking ephemeris provided by the host spacecraft operator is also input into the Kalman Filter. The state vector estimates for each TEMPO dwell time can be used to determine the Earth locations of each of its pixels in real time. Using attitude data to stabilize the TEMPO line-of-sight pointing by providing control inputs into the SMA as described above enables uniform and gapless coverage of the domain. Other than providing ephemeris and gyroscopes, the host spacecraft is only required to orient TEMPO towards the Earth with an accuracy of 1100 μrad (3σ), a capability well within that of a modern commercial communications satellite. Scan tailoring parameters are routinely generated by the INR processing to predict offsets in pointing to keep the TEMPO field of regard centered over a target Earth location. They are applied to the scan starting coordinates in the scan tables defining the data acquisition schedule, which is updated weekly via command uploads. The tailored scan coordinates reduce the need to overcover the domain, making science data collection more efficient.

The tie-point paradigm is that TEMPO and GOES are looking at the same thing, at the same time, and in the same spectral band; therefore, knowledge of the geographic coordinates of unknown features, even clouds, seen by GOES can be transferred to TEMPO. However, it is important to manage the parallax that may arise because TEMPO is not necessarily stationed at a longitude nearby a GOES spacecraft. We do that by either using *a priori* knowledge of object height (cloud top height assignment or topographic height for clear skies) to correct the measured displacement or by binocularly solving for the height of the unknown object by matching it with imagery from two different GOES satellites [95]. The Level 2 requirement is that the angular uncertainty of a fixed point be less than 82 μrad (3σ), 4 km in position on the ground at the center of the field of regard. INR performance for TEMPO is figured to be generally better than 56 μrad (3σ), 2.8 km at the center of the field of regard.

A typical day of operations for TEMPO is shown in Fig. 7. Earth scans are collected with one-hour revisit time during daylight and twilight (two hours before and after full sunlight). The actual daily timeline will vary seasonally, accounting for temperature and stray light. Solar

calibrations may be made when the sun is unobscured at angles $\pm 30°$ to the instrument boresight. Dark frame calibrations are required to support radiometric accuracy. The nominal scan pattern consists of a series of East-West (E-W) scan mirror steps ($\sim$1282) across the field of regard, with the image of the spectrometer slit on the ground defining the North–South extent of the FOV. A continuous sub-section of the field of regard may be scanned at shorter revisit time (5–10 min) for episodic pollution events or focused studies.

Science data collection may be optimized in the early morning and late afternoon when significant portions of the field of regard have solar zenith angles (SZAs) $> 80°$. Data with SZA $> 80°$ are unsuitable for most of the planned atmospheric chemistry measurements, but can constitute 20% of the data collected with the nominal coast-to-coast hourly scanning. The morning optimized data collection will terminate the nominal E-W scan pattern when the SZA $> 80°$ throughout the FOV (governed mainly by the SZA at the southern extent of the FOV), and proceed back to the East-most portion of the field of regard to commence a new E-W scan. Since the entire field of regard is not scanned, the revisit time is less than the nominal 1-h (as small as 5 min) as the scan termination point follows the terminator (SZA $> 80°$) across greater North America. In the afternoon, as the evening terminator progresses westward across the field of regard, data collection will use multiple scan tables to essentially move the initial point of the scan, skipping FOVs with SZA $> 80°$.

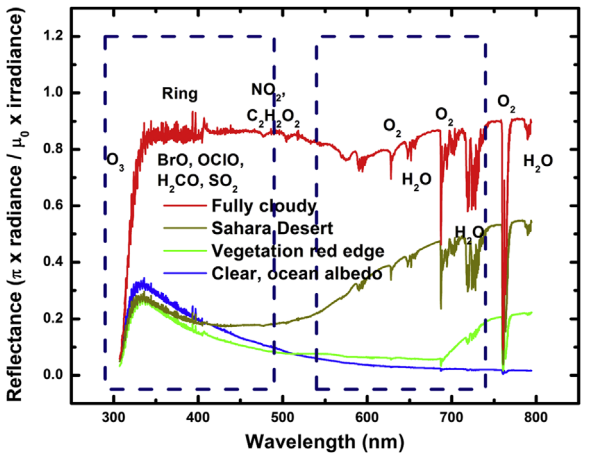

Fig. 5. The spectral regions to be measured by TEMPO are illustrated with reflectance spectra for the range of surface and atmosphere scenes using reflectances derives from European Space Agency GOME-1 measurements. The dashed blue boxes indicate the TEMPO spectral coverage.

4. TEMPO implementation

TEMPO consists of two separate projects: the TEMPO Instrument Project (IP), the competitively selected Earth Venture Instrument project, and the TEMPO Mission Project (MP), directed from the NASA Langley Research Center (LaRC), which provides the spacecraft, integration, and launch.

The TEMPO space segment consists of the TEMPO instrument and the host spacecraft. The host spacecraft vendor is responsible for the integration of the TEMPO instrument to the host spacecraft. The ground segment consists of the Instrument Operations Center (IOC) and the interface to the host Spacecraft Operations Center (SOC). The science segment includes the Science Data Processing Center (SDPC). The ground segment commands the instrument, monitors instrument health and status telemetry, and to receive and transfer science data from the instrument to the IOC and SDPC. The SDPC receives science and telemetry data from the IOC, performs all data processing needed to generate science products, and distributes data products including transmitting all data and products for archival.

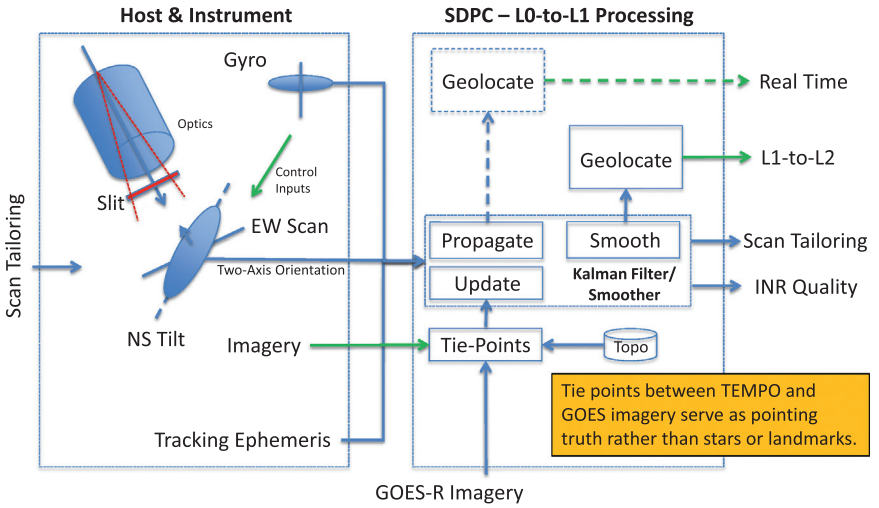

Fig. 6. The TEMPO INR solution creates a Level-1 (L1) product with geographic metadata for each pixel using smoothed Kalman Filter states. Scan tailoring coefficients compensate for deterministic pointing errors to assure efficient coverage of Greater North America.

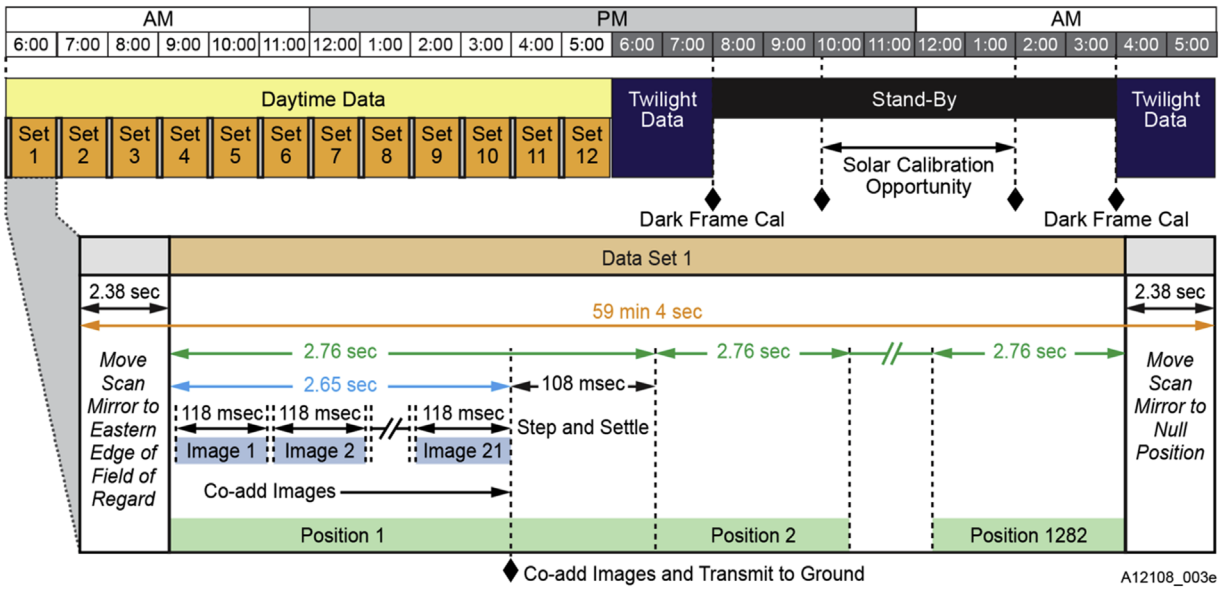

Fig. 7. Nominal daily operations for TEMPO instrument.

4.1. Mission project management

The MP will acquire and manage host accommodations for TEMPO on a commercial GEO spacecraft. The host accommodations provide all the services necessary to enable the instrument on-orbit operations. These include instrument-to-host-spacecraft integration and test, launch services, transfer to GEO, spacecraft operations provided by the host's SOC, delivery of instrument data to the IOC at Smithsonian Astrophysical Observatory (SAO), and support during commissioning and operations.

Host selection will not occur until the instrument is completed. The MP has been working with the potential vendors to reduce the risk that the instrument interface and operational requirements may not be fully met by the host. Using mission accommodation information contained in the Geostationary Common Instrument Interface Guidelines Document as well as information obtained through special studies conducted with host candidates has mitigated this risk. The MP has proposed interface design details to inform the instrument development.

4.2. Instrument project management

The TEMPO IP includes SAO, LaRC, and BATC. The Principal Investigator (PI, K. Chance of SAO) is responsible for the overall project, managing the science, technical, cost and schedule performance. He leads the Science Team and the development of the algorithms, validation, and data processing. He has an Investigation Advisory Panel that includes a senior manager from each partner organization to address organizational issues and a Science Advisory Panel representing international collaborators of the CEOS-recommended international constellation. SAO develops the IOC and the SDPC. The PI has delegated Project Management, Systems Engineering, Safety and Mission Assurance, and management of the BATC prime contract to LaRC.

5. TEMPO operations

5.1. TEMPO ground system

The TEMPO ground system commands the instrument, monitors instrument health and status, and produces Level-0 science data for delivery to the SDPC. TEMPO instrument telemetry is downlinked to the hosts's SOC and then forwarded to the TEMPO IOC, where the telemetry packets are decommutated and processed to Level 0. The IOC autonomously limit-checks the instrument health and status (H&S) data and alerts the operators of any out-of-limit conditions. The H&S data are stored in the IOC for the life of the mission to support remote monitoring, trending, and anomaly resolution. The web-based remote monitoring system allows the operators to graphically view the H&S data in real time and to create plots of the data over arbitrary time intervals. The IOC extracts image data from the telemetry packets to reconstruct CCD image frames. The reconstructed images are sent to the SDPC for assembly into granules for further processing. The IOC also sends gyroscope and scan mechanism controller data to the SDPC to support image pixel geolocation. The commanding component of the IOC utilizes the Ball Aerospace COSMOS command and telemetry system in conjunction with the instrument simulator for command planning, generation, and validation. TEMPO operates from a 14-day command sequence that controls the day-to-day scanning and calibration activities. New 14-day command sequences that incorporate the latest predicted ephemeris and scan tailoring information from INR processing are developed and uplinked on a weekly basis. In the event of a

special observation, the currently executing command sequence can be interrupted and replaced.

5.2. Data processing and availability

The TEMPO instrument operations center at SAO receives telemetry from the host spacecraft operations center. Level 0 science data are passed to the TEMPO SDPC for processing and distribution. In the SDPC, Level 0 data from radiance scans are gathered into granules having sufficient east-west coverage to enable geolocation, typically about 5 min of scan data. Initial radiometric calibration converts the Level 0 digital numbers into physical units, including a stray light correction, and an initial wavelength calibration. When initial radiometric calibration is complete, INR processing derives the latitude-longitude coordinates of the center and corners of each pixel. Knowledge of the scattering geometry facilitates the polarization correction that is applied in producing the final Level 1 radiance spectra. An irradiance spectrum is acquired each night when the sun is 30 degrees from the boresight, usually about two hours before midnight. Consistent irradiance measurement geometry reduces variability associated with angular dependence of the diffuser bidirectional transmittance distribution function. For each Level 1 radiance granule, the Level 2 cloud product is generated first, then the other Level 2 products are generated using the cloud product as input along with the most recent irradiance measurement. The computational cost of the Level 2 ozone profile product is much greater than that of the other Level 2 data products. For this reason, the Level 2 ozone profile product is generated by first coarsely binning each radiance granule, then dividing each granule into many small blocks (e.g. 64 blocks), and processing the small blocks in parallel. Level 3 data products are generated by gridding hourly scans of level 2 data products to standard longitude-latitude grid cells (except the cloud product). All TEMPO data products are stored in netCDF4/HDF-5 format in a data archive at SAO for the life of the mission.

New data products are made available from a website at SAO where data products are organized by date and product type. The website provides access to the most recent 30 days of TEMPO data. Throughout the mission, new data products are regularly (e.g. weekly) transferred to NASA's Atmospheric Science Data Center for public distribution. To facilitate browsing and subsetting, TEMPO data are also made available through the Environmental Protection Agency's Remote Sensing Information Gateway (RSIG).

6. Global constellation and international partnerships

TEMPO is part of a virtual satellite constellation, fulfilling the vision of the Integrated Global Observing System (IGOS) for a comprehensive measurement strategy for atmospheric composition [40]. TEMPO team members have been key participants in international activities to define this potential under the auspices of the Committee on Earth Observation Satellites (CEOS) [14], and as members of Korean and European mission science teams. The constellation will become a reality in the 2020 time frame, including regional geostationary observations over the Americas (TEMPO), Europe (Sentinel-4), and Asia (GEMS) combined with low Earth orbit (Sentinel-5/5P) observations to provide full global context. Mission team members are now working together on data harmonization activities, featuring common data standards and validation strategies, to provide truly interoperable data products from this satellite constellation.

6.1. Europe (Sentinel-4, S4)

The S4 mission, expected launch in 2021, together with Sentinel-5 and the Sentinel-5 Precursor missions, is part of the Copernicus Space Component dedicated to atmospheric composition. The objective of the S4 mission is to provide hourly tropospheric composition data mainly on an operational basis in support of the air quality applications of the Copernicus Atmosphere Monitoring Services over Europe [42,113].

The S4 instrument is a UV/Vis/near infrared spectrometer (S4/UVN) that will fly on the geostationary Meteosat Third Generation-Sounder (MTG-S) platforms in order to measure Earth radiance and solar irradiance. The S4/UVN instrument measures from 305 nm to 500 nm with a spectral resolution of 0.5 nm, and from 750 nm to 775 nm with a spectral resolution of 0.12 nm, in combination with low polarization sensitivity and high radiometric accuracy. The instrument observes Europe with a revisit time of one hour. The spatial sampling distance varies across the geographic coverage area and is 8 km at the reference location at 45°N.

ESA is responsible for the development of the S4/UVN instrument, the Level 1b Prototype Processor (L1bPP), and the Level 2 Operational Processor (L2OP). Instrument and L1bPP are built by a consortium led by Airbus Defence and Space [35]. The L2OP is developed by a consortium led by DLR. It covers key air quality parameters including tropospheric amounts of NO_2, O_3, SO_2, H_2CO, and $C_2H_2O_2$, as well as aerosols, clouds, and surface parameters. Two S4/UVN instruments are expected to be flown in sequence spanning an expected mission lifetime of 15 years. EUMETSAT operates the instrument and processes the mission data up to Level 2.

6.2. Korea (Geostationary Environment Monitoring Spectrometer, GEMS)

GEMS is a scanning UV/Vis imaging spectrometer planned for launch into geostationary orbit in 2019 over Asia to measure tropospheric column amounts of O_3, NO_2, H_2CO, SO_2 and aerosol at high temporal and spatial resolution. With the recent developments in remote sensing with UV/Vis spectrometers, vertical profiles of O_3 (e.g. [67] and centroid height of aerosols (e.g. [85] can be retrieved as well. The required precisions of the products are comparable to those of TEMPO and S4. GEMS is a step-and-stare scanning UV–visible imaging spectrometer, with scanning Schmidt telescope and Offner spectrometer, similar but not identical to TEMPO. The spectral coverage

of GEMS is from 300 nm to 500 nm, with the resolution of 0.6 nm, sampled at 0.2 nm. A UV-enhanced 2D CCD takes images, with one axis spectral and the other north-south (NS) spatial, scanning from east to west (EW) over time. GEMS covers important regions in Asia including Seoul, Beijing, Shanghai, and Tokyo from 5°S to 45°N in latitude, and from 75°E to 145°E in longitude, with the spatial resolution of 7 km (NS) × 8 km (EW) at Seoul. The planned minimum mission lifetime is 7 years.

On orbit calibrations are planned, making daily solar measurements and weekly LED light source linearity checks. For the solar calibration, there are two transmissive diffusers, a daily working one and a reference diffuser used twice a year to check the degradation of the working one. Dark current measurements are planned twice a day, before and after the daytime imaging. In order to avoid dark current issues and random telegraph signal (RTS), the CCD is cooled to −20 °C. Spectral stability is required to be better than 0.02 nm over daily observation hours, stray light less than 2%, polarization sensitivity less than 2% at the instrument level, and the instrument system level MTF better than 0.3 Nyquist.

6.3. Canada

TEMPO provides a unique opportunity to provide consistent and timely air quality information to over 99.5% of the Canadian population. TEMPO data are of particular interest to Canada given the challenges in observing its vast land area from ground-based measurements alone. A primary application of TEMPO data is assimilation into the Environment Canada (EC) air quality forecast system for the purpose of improving air quality forecasts over a domain that largely overlaps with the TEMPO field of regard. Other priority application areas include environmental assessment, epidemiological analyses, health impact studies, and monitoring of natural disasters such as forest fires.

To fully exploit TEMPO, Canada is interested in enhancing TEMPO data quality at higher latitudes where: larger average solar and viewing angles lead to reduced sensitivity of some gases (e.g., O_3 and NO_2) to the boundary layer; stratospheric abundances of some absorbers (also O_3 and NO_2) are larger and display greater variability thereby making them more difficult to remove; TEMPO pixel sizes are larger than at lower latitudes; and where trace gas retrievals in forest fires are complicated by high aerosol loading. Issues in the representation of snow-covered surfaces also lead to larger uncertainties [82]. Canadian academia and government are collaborating to address these by developing direct inversions [80] to improve sensitivity in the boundary layer [29], developing methods to better constrain stratospheric abundances including assimilation of stratospheric profiles, implementing an improved representation of snow in the inversions [74], and developing algorithms to explicitly account for the effects of aerosols on trace gas retrievals [64]. Validation of TEMPO observations over Canada is also a priority with an expansion of the Canadian Pandora network [37] and an aircraft measurement campaign being planned.

6.4. Mexico

The TEMPO field of regard will cover at least 78% of the Mexican territory, including the Mexico City Metropolitan Area with its 21 million inhabitants. Mexico City is one of the best-monitored urban areas in the world with an air quality network (GDF-SEDEMA) run by the city government that has records beginning in 1986 and is now comprised of over 30 stations. Most of these stations measure air pollutants (e.g. O_3, CO, NO_x, SO_2, PM2.5) continuously and are used to advise the authorities when additional measures need to be taken in case of critical pollution events and research purposes. Other large cities with air quality measurements include Monterrey, Guadalajara, Toluca, Tijuana and Mexicali but most of the country lacks information to assess the impacts of air pollution [41]. Therefore, the national environmental institute Instituto Nacional de Ecología y Cambio Climático (INECC) and SAO have signed a memorandum of understanding in order to work towards making the data produced by TEMPO available and useful for the Mexican public.

A strong academic collaboration has been established with the National Autonomous University of Mexico (UNAM). Together with other institutions and universities, a nationwide network of atmospheric observatories (RUOA) has been established to continuously measure additional species including black carbon and greenhouse gases. A network of four MAX-DOAS instruments has been installed in Mexico City [3] producing NO_2 and H_2CO total vertical columns with high temporal resolution. The data produced in Mexico City and other locations will be part of the validation efforts of TEMPO.

The TEMPO observations over Mexico are of particular interest to better characterize emissions from industrial and urban regions which are poorly studied. Biomass-burning sources particularly during the distinctive dry season and the harmful agricultural practices in many parts of the country are monitored by TEMPO. This will be of great value to alert vulnerable communities and prevent damages as well as to increase the understanding of the variability and dynamics of transported pollution plumes.

7. TEMPO science products

7.1. Standard data products

TEMPO will measure as standard data products the quantities listed in Table 2 for greater North America. The O_3 products, NO_2, and H_2CO are required products and meet precision requirements up to 70° SZA. The spatial and temporal resolutions and SZA constraints are for meeting the requirements only. Operational retrievals will be done hourly at native spatial resolution ($\sim 2.1 \times 4.4\ km^2$) during the day-lit period except for ozone profile retrievals at the required spatial resolution of $\sim 8.4 \times 4.4\ km^2$ (four co-added pixels for increased signal and reduction of computational resources). Precisions are listed for all species for four co-added pixels, as that is the form of the NASA precision requirements for the mission.

Table 2.
TEMPO standard data products.

Species/Products		Typical value[a]	Required precision[a]
O_3 Profile	0-2 km (ppbv)	40	10
	FT (ppbv)[b]	50	10
	SOC[b]	8×10^3	5%
Total O_3		9×10^3	3%
NO_2[c]		6	1.00
H_2CO[c] (3 measurements per day)		10	10.0
SO_2[c] (3/day)		10	N/A
$C_2H_2O_2$ (3/day)		0.2	N/A
H_2O		3×10^8	N/A
BrO		5×10^{-2}	N/A
AOD		$0.1-1$	0.05
AAOD		$0-0.05$	0.03
Aerosol Index (AI)		-1 to $+5$	0.2
Cloud Fraction		$0-1$	0.05
Cloud Top Pressure (hPa)		$200-900$	100

Spatial resolution: 8.4×4.4 km^2 at the center of the field of regard. Time resolution: Hourly unless noted.
[2]Expected precision is viewing condition dependent. Results are for nominal cases.
UV indices, including the erythemally weighted irradiance are derived from O_3 and other parameters.
[a] Units are 10^{15} molecules cm^{-2} for gases and unitless for aerosols and clouds unless specified.
[b] FT = free troposphere, 2 km – tropopause; SOC – stratospheric O_3 column.
[c] Background value. Pollution is higher, and in starred constituents, the precision is applied to polluted cases.

7.2. Additional data products

Volcanic SO_2 (column amount and plume altitude) and diurnal out-going shortwave radiation and cloud forcing are potential research products. Additional cloud/aerosol products are possible using the O_2-O_2 collision complex and/or the O_2 *B* band. Additional aerosol products will combine measurements from TEMPO and GOES-R. Nighttime "city lights" products, which represent anthropogenic activities at the same spatial resolution as air quality products, may be produced twice per day (late evening and early morning) as a research product. Meeting TEMPO measurement requirements for NO_2 (visible) implies the sensitivity for city lights products over the CONUS within a 2-h period at 8.4×4.4 km^2 to 4.25×10^{-9} W cm^{-2} sr^{-1} nm^{-1}.

7.3. TEMPO retrieval sensitivity study

Trace gas retrieval sensitivity has a key role in the determination of TEMPO instrument requirements to guide the design and the verification of the TEMPO instrument performance. It is a two-step process: We first perform radiative transfer model (RTM) simulations of TEMPO radiance spectra and weighting functions (or Jacobians) using the VLIDORT radiative transfer model [98] and then conduct calculations of retrieval errors for various trace gases using the optimal estimation approach.

To represent the retrieval performance of TEMPO hourly measurements throughout the year, we use hourly fields of GEOS-Chem model (v9-01-01) simulations [70] and its associated GEOS-5 meteorological data at 2.5° longitude $\times$ 2° latitude for 12 days (15th of each month) in 2007 over the TEMPO field of regard. Although this is a much coarser horizontal resolution than the TEMPO footprint, our focus here is on the performance for vertical columns and profiles. The model fields include profiles of temperature, relative humidity, tropospheric O_3, NO_2, H_2CO, SO_2, $C_2H_2O_2$, extinction coefficients for six types of aerosols (dust, sulfate, organic carbon, black carbon, coarse sea salt and fine sea salt), clouds, and cloud fraction. Profiles of H_2O mixing ratio are derived from relative humidity and temperature fields. The tropospheric O_3 profiles are appended to stratospheric O_3 profiles from OMI retrievals [65]. The NO_2 profiles are appended to stratospheric NO_2 profiles from PRATMO simulations. Stratospheric BrO and OClO profiles (down to 10 km) are also from PRATMO simulations [75] and are extended to the surface from 10 km by assuming constant mixing ratio. Profiles of air number densities, O_2, O_2–O_2 are derived from temperature/pressure fields. A total of 10 trace gases are considered in the calculation. Viewing geometries for each scene are computed based on TEMPO viewing for a given satellite longitude (e.g., 100°W). Surface albedo is based on the GOME albedo database [58], which provides monthly mean surface albedo climatology at a spatial resolution of $1^\circ\times1^\circ$ for 11 1-nm-wide wavelength from 335 nm to 772 nm, and is interpolated or extrapolated to TEMPO wavelengths. The independent pixel approximation is assumed for partial cloudy conditions. TEMPO radiance spectra (290–490 nm, 540–740 nm) and corresponding weighting functions with respect to trace gases, aerosols (optical depth and single scattering albedo), clouds (optical depth, cloud fraction), and surface albedo are calculated with VLIDORT at a spectral resolution of 0.6 nm FWHM and spectral intervals of 0.2 nm for scenes with solar zenith angle $\leq$ 80°. About 90,000 atmospheric scenarios are simulated, with ~23,000 nearly clear-sky scenes with cloud fraction $\leq$10% used in the retrieval sensitivity analysis.

We use optimal estimation (OE) [89] to conduct retrieval sensitivity analysis for both ozone profile and trace gas retrievals. Let $\mathbf{x}$ be the state vector, the vector of values to be retrieved by the observation, and let $\mathbf{y}$ be the observed radiances. The solution error covariance matrix $\hat{\mathbf{S}}$ can be derived as follows without doing actual iterative non-linear retrievals:

$$\hat{\mathbf{S}}=(\mathbf{K}^{\mathbf{T}}\mathbf{S}_{\mathbf{yn}}^{-1}\mathbf{K}+\mathbf{S}_a^{-1})^{-1} \quad (1)$$

$\mathbf{K}=\partial\mathbf{y}/\partial\mathbf{x}$ is the weighting function matrix, $\mathbf{S}_{\mathrm{yn}}$ is the measurement random-noise error covariance matrix, and $\mathbf{S_a}$ is the *a priori* error covariance matrix. To make the problem more linear, $\mathbf{y}$ is taken as the logarithm of normalized radiance ($\mathbf{R}=\mathbf{I}/\mathbf{F}$), in which $\mathbf{I}$ is the radiance and $\mathbf{F}$ is the solar irradiance. For profile retrievals, a very useful quantity to characterize the retrieval sensitivity is the averaging kernel matrix $\mathbf{A}$, defined as:

$$\mathbf{A}=\frac{\partial\hat{\mathbf{x}}}{\partial\mathbf{x}_t}=\hat{\mathbf{S}}\mathbf{K}^{\mathbf{T}}\mathbf{S}_{\mathbf{yn}}^{-1}\mathbf{K}=\mathbf{GK}. \quad (2)$$

$\mathbf{A}$ gives the sensitivity of the retrieved state vector $\hat{\mathbf{x}}$ to the true (but unknown) state vector $\mathbf{x_t}$. $\mathbf{G}$ is the matrix of

contribution functions, $\mathbf{G} = \partial\hat{\mathbf{x}}/\partial\mathbf{y}$. The OE approach of using $\mathbf{S_a}$ to regularize the retrievals is typically used for ill-posed profile retrievals and will be used for TEMPO ozone profile retrievals. TEMPO trace gas retrieval algorithms are based on a two-step approach, first performing non-linear least squares (NLLS) fitting to derive slant column densities (SCDs), and then calculating air mass factor (AMF) and converting SCDs to vertical column densities (VCDs). However, the OE retrieval error estimate from Eq. (1) converges to that of NLLS if $\mathbf{S_a^{-1}}$ approaches zero, i.e., using it as a very loose constraint. Furthermore, for the retrieval of VCD for a given trace gas using Eq. (1) allows direct estimate of VCD retrieval errors by implicitly taking the AMF into account.

Table 3.
Statistics (mean and 1σ) of retrieval precisions and errors for various products, and the percentage of scenarios meeting the requirements (MR).

Product[a]	Precision	Total errors	Meets reqs. (%)
UV total O_3	0.32 ± 0.08	0.72 ± 0.08	100
UV trop. O_3	3.05 ± 0.71	6.38 ± 1.98	98.3
UV 0-2 km O_3	2.59 ± 0.70	8.86 ± 1.53	78.2
UV/Vis total O_3	0.30 ± 0.07	0.54 ± 0.13	99.4
UV/Vis trop. O_3	3.04 ± 0.90	5.21 ± 1.72	98.9
UV/Vis 0–2 km O_3	3.29 ± 0.71	7.93 ± 1.41	92.8
NO_2 ($\times 10^{15}$)	0.30 ± 0.08	0.36 ± 0.20	98.4
H_2CO ($\times 10^{16}$)	0.38 ± 0.10	0.42 ± 0.13	100
$C_2H_2O_2$ ($\times 10^{14}$)	4.68 ± 1.56	4.75 ± 1.62	N/A
SO_2 ($\times 10^{16}$)	1.09 ± 0.49	1.86 ± 1.04	N/A

[a] The units are % for total ozone column, ppbv for tropospheric O_3 and 0–2 km O_3, and molecules cm^{-2} for other trace gases.

Table 3 summarizes the conclusion of the sensitivity study. As measurement requirements cannot always be met for every atmospheric scenario, we have defined that requirements are met if the percentage of atmospheric scenarios meeting the baseline requirements is above a certain threshold. The threshold is 95% for NO_2 and H_2CO, but 90% for O_3. From Table 3, measuring 0-2 km O_3 will likely pose the biggest challenge. Even so, if TEMPO can meet the baseline requirements of measuring 0–2 km O_3 to 10 ppbv precision 78% of the time, the results will be revolutionary.

7.4. O_3 profile retrieval algorithm

The TEMPO operational ozone profile algorithm is adapted from the SAO ozone profile algorithm that we have developed for GOME [66], OMI [65], and GOME-2 [12]. An updated OMI algorithm as described in [56] is being used to routinely process all the OMI data in the OMI Science Investigator-led Processing Systems (SIPS). Unlike OMI retrievals, the TEMPO retrieval algorithm will combine both UV (290–345 nm) and visible (540–650 nm) measurements to improve retrievals in the lower troposphere [16,79]. This technique will provide revolutionary measurements of ozone air quality. Fig. 8 is an illustration using averaging kernels of the benefit of including visible

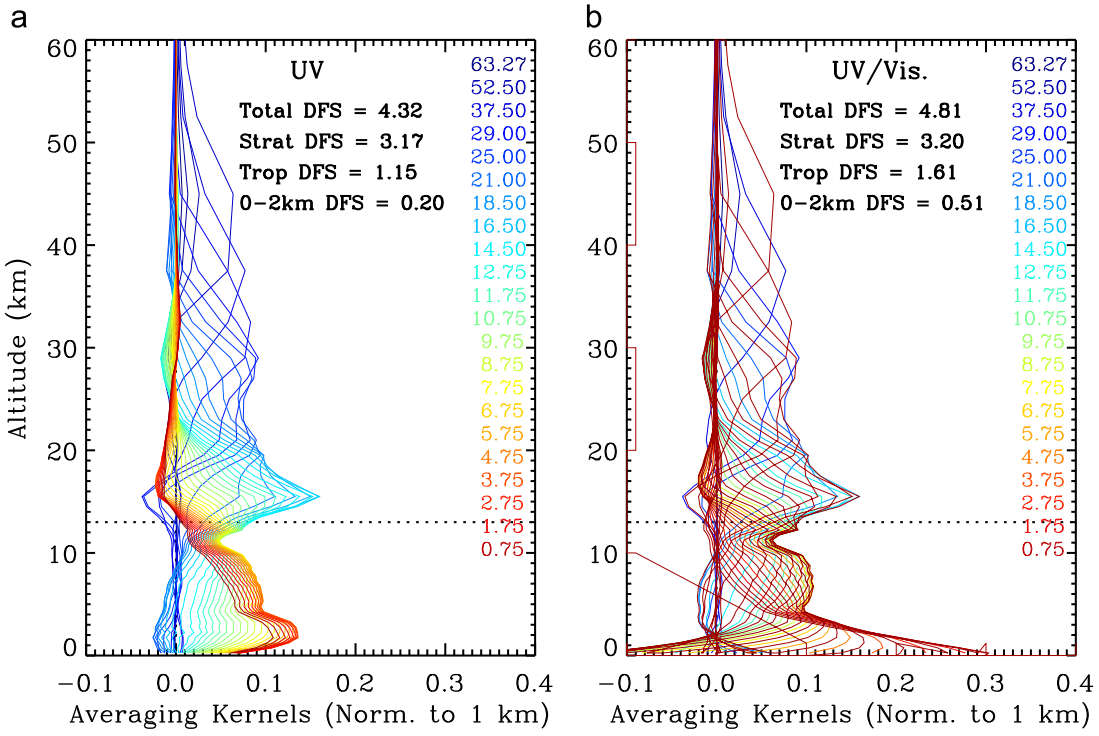

Fig. 8. Rows of two averaging kernel matrices based on iterative nonlinear retrievals from synthetic TEMPO radiances with the signal to noise ratio (SNR) estimated using the TEMPO SNR model at instrument critical design review in June 2015 for (a) UV (290–345 nm) retrievals and (b) UV/Visible (290–345 nm, 540–650 nm) retrievals for clear-sky condition and vegetation surface with solar zenith angle 25°, viewing zenith angle 45° and relative azimuthal angle 86°. DFS is degrees of freedom for signal, the trace of the averaging kernel matrix, which is an indicator of the number of pieces of independent information in the solution.

wavelengths to the profile retrieval. The enhancement in sensitivity in the lowest 2 km of the troposphere is provided by the increased penetration of the solar irradiance to altitudes near the surface. As 0–2 km O_3 is a key baseline requirement for TEMPO, we will add more layers in the troposphere and add the output of 0–2 km ozone column and corresponding retrieval uncertainties derived from the profile retrieval covariance matrix. Hourly meteorological data of temperature profiles, surface and tropopause pressure from the North America Mesoscale Forecast system (NAM), with nest output grid of 5.0 km Lambert Conformal (http://www.emc.ncep.noaa.gov/mmb/namgrids), integrated over the continental United States (CONUS) is planned to be used to set up the atmosphere and better account for the temperature dependence of trace gas absorption. The climatological a priori will be based on the recent tropopause-based ozone profile climatology [5]. As the UV/Vis joint retrieval has not been demonstrated from actual measurements, we are using GOME-2 data to test this joint retrieval concept to reduce the science risk. The UV/Vis ozone profile algorithm has been mostly implemented for GOME-2 retrievals [64].

Due to the weakness of ozone absorption features in the visible [8] the combined UV/Vis measurement is highly sensitive to the visible surface reflectance. [128] used reflectance spectra from three different reflectance databases to capture the range of different surface reflectance spectra through an Empirical Orthogonal Function (EOF) analysis. This information was combined with satellite reflectance products that inform the surface reflectance at discrete wavelengths for each given scene to generate a climatology of geometry dependent surface reflectance spectra. To assist validation of this reflectance climatology and characterize reflectance of the land cover types at TEMPO resolutions, synchronous field and airborne data collection campaigns in the St Louis Metro region were performed. We have collected spectral reflectance data of various land cover types on the ground within hours of a GeoTASO [81] overpass using a field-based hyperspectral spectroradiometer and used GeoTASO data for spectral albedo measurements to develop a spectral albedo database of various land cover types found in Midwestern US.

In addition, we will use the latest HITRAN database to account for the temperature and pressure dependence of O_2 and H_2O in the visible region and use O_2–O_2 cross sections by Thalman and Volkamer [102] to account for the temperature dependence of O_2–O_2 absorption. However, the GOME-2 data are not optimized for UV/Vis retrievals as the peak of visible Chappuis bands is split into two channels. Consistent radiometric calibration among different channels is also critical to the joint retrievals. We are still working on the improvement of GOME-2 radiometric calibration towards the demonstration of joint UV/Visible retrievals. In case the UV/Vis retrieval algorithm does not provide the expected performance, we can run the operational algorithm using UV measurements only. Ozone profile and tropospheric ozone retrievals are led in Europe for S4 by the Rutherford Appleton Laboratory, who also participates in the TEMPO Science Team. Their innovative development in algorithm physics fitting approach [76] are available for TEMPO studies as part of our long-term collaboration.

7.5. Radiative transfer modeling

Radiative transfer (RT) calculations for TEMPO are carried out with the widely used linearized RT model VLIDORT [97]. This is an accurate full multiple-scattering polarized RT code for use in optically-stratified (multilayer) one-dimensional scattering media. VLIDORT uses the discrete ordinate solution method to solve the vector radiative transfer equation in each layer. VLIDORT has been validated against benchmark results in the literature and is a free-to-use code in the public domain. It will be necessary to speed up multiple-scatter RT simulations when performing TEMPO ozone profile retrievals, since VLIDORT is a computationally intensive RT model, particularly when running with polarization included. A recently-developed performance-enhancement scheme, based on PCA (principal component analysis) applied to hyperspectral optical property data sets, will be deployed to speed up calculations of radiance and Jacobians [96].

7.6. Trace gas column measurements

TEMPO operational trace gas retrievals are based on a two-step approach widely employed for optically thin trace gas retrievals in the UV and visible spectral range [103,19,55,88]. The first step consists in the determination of slant column densities (SCDs) representing the integrated number density of trace gas molecules in the mean photon path from the sun to the instrument by direct fit of radiance spectra [17]. The second step consists in the calculation of VCDs using AMFs calculated offline with a radiative transfer model [84].

Nitrogen dioxide The high spatial and temporal resolution of TEMPO is of particular benefit for NO_2 in the boundary layer given its high heterogeneity due to spatially and temporally varying sources together with the short NO_x lifetime. The TEMPO NO_2 algorithm will build on retrieval algorithms developed for previous UV/Vis instruments [109,62,7,71,87]. State-of-the-science retrieval algorithms consist of a spectral fit of NO_2 to a selected wavelength window of a measured radiance spectrum to determine the slant column density (SCD, which represents the integrated abundance of NO_2 along the average photon path through the atmosphere) algorithm in the 400–465 nm wavelength range, calculation of an air mass factor (AMF) to convert the SCD into a vertical column density (VCD), and a scheme to separate stratospheric and tropospheric components. To properly remove stratospheric NO_2 from the total retrieved NO_2 column in order to generate accurate tropospheric columns, TEMPO will employ a modified approach described in [10], using near local observations over unpolluted and cloudy areas. Alternatively, the stratospheric NO_2 field can be generated by a data assimilation scheme (e.g. [7,23]), provided real time NO_2 forecasts are available at TEMPO processing time. The resultant TEMPO NO_2 will offer a powerful constraint on NO_x emissions [72,100].

Formaldehyde H_2CO is one of the most abundant non-methane volatile organic compounds (NMVOCs) in the troposphere and is an important atmospheric trace gas due to its involvement in the chemical pathways of tropospheric ozone formation and in the relationship with the concentration of hydroxyl radicals (OH), the main tropospheric oxidant [2]. Continental hot spots are consequence of the oxidation of short-lived NMVOCs from anthropogenic, biogenic, and pyrogenic origins as well as direct emissions from fires and industrial activities [127,33,70]. Due to its high reactivity it has a short tropospheric lifetime of few hours [9] making it a useful proxy for NMVOCs emissions in satellite observations and for the estimation of top-down emission inventories of isoprene [6,83]. The H_2CO TEMPO operational retrieval is based in the experience accumulated over the last decades, starting with the [19] retrieval of H_2CO from GOME-1. Since then, H_2CO retrievals have been made using data from SCIAMACHY, OMI, GOME-2 and OMPS [21,22,31,32].

Sulfur dioxide Operational SO_2 will be produced at launch using the two-step method. Two additional methods will be studied for later retrievals. One method is the principal component analysis (PCA) algorithm [63] where a set of principal components (PCs) is directly extracted from satellite-measured radiances taken over SO_2-free regions. By fitting these PCs along with the SO_2 Jacobians (i.e., the sensitivities of satellite-measured radiances to given perturbations in SO_2 VCD) to the measured radiances SO_2 loading is determined. The PCA algorithm has been successfully implemented with several polar-orbiting sensors including OMI, OMPS, TOMS, and GOME-2 and is now the operational algorithm for the new generation OMI standard planetary boundary layer (PBL) SO_2 product [28]. The other method is the SAO SO_2 optimal estimation algorithm [80], which was developed to retrieve SO_2 vertical columns simultaneously with ozone profiles. The optimal estimation approach applies the ozone profile algorithm for SO_2, using an online radiative transfer calculation and trace gas climatologies to include the effects of surface albedo, clouds, ozone and SO_2 profiles in the retrieval.

Glyoxal Operational $C_2H_2O_2$ will be produced at launch using the two-step method. It is a short lived product of non-methane volatile organic compound oxidation. Along with formaldehyde, TEMPO glyoxal observations will be critical for understanding the impact of isoprene on atmospheric chemistry, particularly in the southeastern United States where emissions are high. Current models suggest that glyoxal formed through isoprene oxidation accounts for 28% of isoprene-derived SOA [69]. Recent work has shown that the H_2CO yield from isoprene oxidation has a strong NO_x dependence [70,122]. Determining the NO_x dependence of $C_2H_2O_2$ will be critical for interpreting satellite observations. TEMPO will resolve a wide range of NO_x regimes due to its high spatial resolution, making NO_2, H_2CO and $C_2H_2O_2$ crucial datasets for validating isoprene chemistry. The ratio of $C_2H_2O_2$ to H_2CO can provide insight on the VOC speciation and dominant chemical pathways in different locations [54]. Satellite $C_2H_2O_2$ retrievals are a good aromatic emissions constraint where these are high [15,68]. Within the TEMPO field of regard, high aromatic concentrations have been observed in cities including Mexico City [44,114] and Los Angeles [121], and oil and gas fields such as the Uintah Basin [36].

Water vapor Operational H_2O will be produced at launch using the two-step method. Recently, the $430-480$ nm spectral region, where H_2O is a weak absorber, has been used to retrieve water vapor slant columns from GOME-2 and OMI spectra [115]; H. [116,120]. Water vapor retrieved from the visible spectrum has good sensitivity to the planetary boundary layer, since the absorption is optically thin, and is available over both the land and ocean. The hourly coverage of TEMPO will greatly improve the knowledge of water vapor's diurnal cycle and make rapid variations in time readily observed.

BrO and IO BrO was first measured from space with the ESA GOME-1 instrument after predictions of global measurements [17,18]. Observations are ongoing and global, from current and past LEO UV/Vis instruments. Studies of enhancements in polar regions are particularly well-developed (cf. [20]. Operational BrO will be produced at launch using the two-step method, assuming stratospheric AMFs [17]. Scientific studies will correct retrievals for tropospheric content. IO was first measured from space using SCIAMACHY spectra [90]. It will be produced as a scientific product using the two-step method, particularly for coastal studies, assuming AMFs appropriate to lower tropospheric loading.

Aerosols TEMPO's operational algorithm for retrieving aerosols will be based upon the OMI's aerosol algorithm that uses the sensitivity of near-UV observations to particle absorption to retrieve aerosol absorption properties in conjunction with the aerosol extinction optical depth. In addition to the qualitative Absorbing Aerosol Index (AAI), TEMPO will derive aerosol optical depth (AOD) and single scattering albedo (SSA) using an algorithm similar to that currently applied to OMI observations, known as OMAERUV [104,105]. In this algorithm, observations at 354 and 388 nm are used as input to retrieve the AOD and SSA parameters. Aerosol heights are based on a climatology derived from CALIOP (Cloud-Aerosol Lidar with Orthogonal Polarization) measurements. At the TEMPO footprint size, the finest to date for UV/Vis spectrometers, sub-pixel cloud contamination will be less of a problem than it was for OMI. The algorithm uses forward radiative transfer calculations of upwelling reflectances at the top of the atmosphere associated with three aerosol types: carbonaceous, desert dust, and urban/industrial particulate. Because the retrieval of UV-absorbing aerosols is sensitive to aerosol layer height, when dealing with elevated layers of carbonaceous or desert dust aerosols it is necessary to account for the height effect.

As the first geostationary satellite to measure UV/Vis spectra over North-America, TEMPO provides a unique opportunity to develop new research algorithms for aerosol retrievals by taking advantage of its hourly observations and its synergy with other geostationary satellites that measure the radiation in the visible, shortwave infrared and thermal infrared. Based on spectra collected by GeoTASO [81], Hou et al. [39] have developed a theoretical framework for multispectral retrieval of aerosol properties. GeoTASO is a test-bed instrument for TEMPO

and was designed for analogous UV/Vis air quality measurements Information content analysis shows that in fine-mode aerosol dominated conditions (which are often the case over North America), the wavelength-dependent AOD and aerosol effective radius can be retrieved accurately [38].

TEMPO may be used together with the Advanced Baseline Imager (ABI) instruments on the NOAA GOES-R and GOES-S satellites for aerosol retrievals ([119]. The ABI will image in 16 different spectral bands including 0.64 μm at 0.5 km spatial resolutions and at 0.47 μm, 0.87 μm and 1.6 μm at 1 km resolution [92]. TEMPO and ABI will view the same scene at two different but constant viewing angles and measure the reflectance at least in two common wavelengths (0.47 and 0.64 μm). J. [116] showed that a combination of 3 shortwave bands from GOES-R (470, 640, and 860 nm) and 4 bands from TEMPO (340, 380, 470, and 640 nm) can improve the retrieval of both AOD and fine-mode AOD accuracy; comparing to the retrieval from the single sensor, the joint retrieval reduces AOD and fine model AOD uncertainties respectively from 30% to 10% and from 40% to 20%. The improvement of AOD is in part due to the much lower surface reflectance in the near-UV (where TEMPO measures) and is especially evident when TEMPO is located in the zenith direction of the sun, the direction for which the surface bidirectional reflectance distribution function (BRDF) is largest (J. [116,123]). Multiple measurements taken for the same pixel (from same viewing angle but multiple solar zenith angle and therefore scattering angles) can provide information on aerosol shape [118]. In addition, the ABIs' 0.5 km cloud mask will be available to identify sub-pixel size clouds in the TEMPO footprint, and AOD derived from ABIs at 0.47μm can be converted to the near UV and used as an input to a modified TEMPO aerosol algorithm that would then use available near UV observations to characterize the aerosol absorption spectral dependence.

Clouds The default cloud algorithm for TEMPO will be based on the rotational Raman scattering (RRS) cloud algorithm that was developed for OMI (known as OMCLDRR) and detailed in [53,48,112]. Rotation Raman scattering (RRS) from atmospheric molecules produces filling and depletion effects in the Earth's backscattered spectrum known as the Ring effect. The spectral effect for a single scattering is a convolution of the rotational Raman spectrum with that of the sun: This has a spectral smoothing effect (*cf.* [52]). There is no RRS from scattering due to cloud and aerosol particles. Therefore, clouds in general reduce the amount of RRS as compared with clear sky. The higher the clouds, the more Rayleigh and Raman scattering are reduced. [45] exploited this fact to retrieve cloud pressures from solar backscatter ultraviolet (SBUV) continuous spectral scan measurements. This approach was fine tuned and applied to other satellite spectrometers including GOME, OMI, and the Ozone Mapping Profiling Suite (OMPS) [110].

The OMCLDRR algorithm makes use of the mixed Lambertian equivalent reflectivity (MLER) model [99]. In the MLER framework, a surface (cloud or ground) is modeled as opaque and Lambertian. In the MLER model, an effective cloud fraction is used to weight the radiance components coming from the clear and cloudy portions of the pixel. The effective cloud fraction is computed using the reflectivity at a wavelength not substantially impacted by RRS or atmospheric absorption. Cloud pressures derived from OMCLDRR and other solar backscatter approaches are much higher (inside the cloud) than the physical cloud top that is provided by thermal infrared measurements [112]. Retrieved cloud pressures from OMCLDRR are not at the geometrical center of the cloud, but rather at the optical centroid pressure (OCP) of the cloud. OCPs can be thought of and modeled as the averaged pressure reached by backscattered photons [50]. Cloud OCPs are the most appropriate cloud pressures for use in trace gas retrievals from the same instruments (e.g., [111,47]). Furthermore, the differences between cloud OCPs and cloud top pressures can be exploited to detect multilayer clouds in combination with thermal infrared measurements [49]. Such an approach can be implemented with data from TEMPO and GOES-R.

There are other instrumental and geophysical effects that can cause filling of solar lines and thus produce errors in cloud pressures derived from RRS if not accounted for. These effects include stray light, dark current, cloud 3D effects, and cloud shadowing. RRS algorithms may be more sensitive to these effects than other approaches to derive cloud pressure. We are therefore developing a backup cloud algorithm for TEMPO based on absorption from the oxygen collision complex (O_2-O_2) at 477 nm. Such an approach was developed [1] and evaluated [94] with OMI data. We are also currently working on upgrades to the OMCLDRR and O_2-O_2 algorithms to better account for surface anisotropy effects over both land and ocean.

Fluorescence and other spectral indicators Global measurements of solar-induced fluorescence (SIF) from chlorophyll over both land and ocean have recently been made with several different satellite instruments. In terrestrial vegetation, chlorophyll fluorescence is emitted at red to far-red wavelengths (~650-800 nm) with two broad peaks near 685 and 740 nm, known as the red and far-red emission features. Oceanic SIF is emitted exclusively in the red feature. SIF measurements have been used for studies of tropical dynamics, primary productivity, the length of carbon uptake period, and drought responses, while ocean measurements have been used to detect red tides and to conduct studies on the physiology, phenology, and productivity of phytoplankton (see [51] and references therein). All SIF measurements to date are from instruments are in polar sun-synchronous orbits with equator crossing times in the morning or early afternoon.

We have simulated thousands of spectra with and without SIF using full monochromatic radiative transfer calculations and have performed retrievals on those spectra and compared with the truth using the approach of [46,51]. Our initial simulations show that TEMPO can retrieve both red and far-red SIF by utilizing the property that SIF fills in solar Fraunhofer and atmospheric absorption lines in backscattered spectra normalized by a reference (e.g., the solar spectrum) that does not contain SIF. Precision can be improved by averaging in time and/or space. The final precision will depend upon the selected

temporal and spatial resolution for averaging that may vary with the desired application.

TEMPO will also be capable of measuring spectral indices or modified indices (to work within the TEMPO spectral range) developed for estimating foliage pigment contents and concentrations (e.g., [108]. Spectral approaches for estimating pigment contents apply generally to leaves and not the full canopy. A single spectrally invariant parameter, the Directional Area Scattering Factor (DASF), relates canopy-measured spectral indices to pigment concentrations at the leaf scale [57]. The DASF retrieval can be retrieved using reflectances in TEMPO's 710–740 nm spectral range [57] and does not require canopy reflectance models or prior information on canopy structure.

UVB TEMPO measurements of daily UV exposures build upon heritage from OMI and TROPOMI measurements. Hourly cloud measurements from TEMPO allow taking into account diurnal cloud variability, which has not been previously possible. The OMI UV algorithm [101] is based on the TOMS UV algorithm [25,59,60]. It consists of a calculation for the clear sky case, with corrections for clouds (or non-absorbing aerosols). Additional correction, which exploits monthly aerosol climatology, is also applied to account for absorbing aerosols [4]. The irradiance product is the result of a radiative transfer model calculation, using the following input parameters: the total ozone column and the scene reflectance at 360 nm (the latter to account for clouds and scattering aerosols). The specific product is the downward spectral irradiance at the ground (in $W\,m^{-2}\,nm^{-1}$) and the erythemally weighted irradiance (in $W\,m^{-2}$). The approach chosen for estimating surface UV irradiances based on TROPOMI measurements builds on the TOMS-OMI heritage, while also utilizing parts of the Offline UV algorithm (OUV) [61]. The inputs for the VLIDORT radiative transfer calculations are the retrieved total ozone column and reflectance at 354 nm together with information on the surface albedo and the atmospheric aerosol loading from other sources. Here, the reflectance at 354 nm is used to determine the cloud optical thickness, assuming a generic water cloud located between 1 and 2 km above the surface.

8. Validation

Validation of TEMPO measurements requires techniques capable of significantly better spatio-temporal characterization of the atmosphere than for previous LEO space-based air-quality observations. At the same time, the fiscal constraints of the Earth Venture Program necessitate creative approaches to the challenges of TEMPO validation, including coordinated federated approaches. The minimum validation effort compares TEMPO baseline products with ground-based correlative data collected from daytime (SZA $< 70°$) observations at least one month each season from at least three ground validation sites in the North America. This effort identifies and corrects regional-scale and diurnal systematic biases in the space-based products and demonstrate required precisions in polluted clear-sky scenes to the levels listed in Table 2. Pandora solar spectral-radiometer measurements [37] are the primary source of correlative data for trace-gas column densities and, where possible, their atmospheric profiles. This approach requires accurate accounting for the vertical sensitivities of both the Pandora and TEMPO trace-gas retrievals. Ozonesondes, co-located with Pandoras, will contribute to the validation of the O_3 products.

One aspect of the validation effort is to measure O_3, NO_2, and H_2CO in observation programs designed to determine their spatial and temporal gradients over the scale of a TEMPO ground pixel. Current long-term Pandora sites include NASA Goddard Space Flight Center, NASA Headquarters, the Smithsonian Environmental Research Center, LaRC, Boulder, CO, Houston, TX, and Four Corners, NM plus several sites in Canada. Additional sites are coming online regularly. There is extensive potential for validation activities involving additional products with correlative measurements and techniques. On a case-by-case basis, as resources allow and opportunities occur, we plan evaluation of TEMPO products beyond the baseline set (e.g., SO_2, $C_2H_2O_2$, cloud products, and aerosol products) and geophysical conditions.

Additional anticipated sources of correlative and validation data sources to help support a more robust validation activity could include 1) surface in-situ-measurement networks; both operational air-quality networks such as State and Local Air Monitoring Stations (SLAMS) and related ambient air networks (PAMS/NCore, CASTNet, CSN, and IMPROVE), along with research networks SPARTAN and $BEACO_2N$, along with Canadian and Mexican assets; 2) surface remote-sensing/profiling networks and research sites: TOLNet, NDACC, Pandora, Ozonesonde, Brewer/Dobson, CAPABLE, AIRS, NAPS (Canada), and Mexican assets; 3) Aircraft excursions and campaigns such as Earth Venture sub-orbital missions; NASA, NOAA, NSF, or EPA campaigns that include TEMPO species and products (e.g., GeoTASO and ACAM/GCAS); and 4) space-borne instruments including OMI, GOME-2, NPP/OMPS, TROPOMI, and Sentinel-5P. These surface in-situ, surface remote-sensing, airborne, and polar-orbiting space-borne instruments comprise a very rich set of potential validation data sources, and TEMPO welcomes collaborations with scientific investigators using these measurements. To properly exploit disparate data sources with differing spatio-temporal resolutions it will be useful to employ chemical models as intercomparison platforms. This methodology has been used previously to compare satellite measurements of ozone [124] and satellite measurements of methane and formaldehyde with in situ data [106,126].

The TEMPO validation team is also fostering collaborations with other science teams, educational institutions, and space-related organizations including the Korean GEMS mission, the European Sentinel 4 and 5 P missions, the NASA/NOAA NPP/OMPS mission, and the Global Space-based Inter-calibration System (GSICS). Although neither GEMS nor Sentinel 4 will provide direct correlative data for TEMPO, maintaining close scientific ties with the scientists on these similar missions will foster consistent results in the constellation. For example, GeoTASO [81] airborne data and 10 Pandora ground stations will be used in the 2016 KORUS campaign for GEMS algorithm

development and are also valuable potential validation data sources for TEMPO.

Preliminary validation activities started in 2015 will proceed throughout the mission with intensive focus from 24 months before launch to 15 months after launch. The preliminary activities include coordinating ground-based assets, developing tools for validation analyses, exercising forward models, and implementing the validation tools. The TEMPO validation team is also engaging with the aircraft and space-borne communities to coordinate potential validation and science campaigns with synergistic potential.

9. Science studies, including special observations

Many important new scientific studies are made possible by the temporal and spatial resolution of TEMPO. We present a selection of them here. It is certainly not nearly exhaustive. Some of these studies benefit from shorter revisit times than the hourly cycle. Substantial measurement time for these high-frequency (likely as short as 10 min) scans of a subsection of the field of regard will be available during the TEMPO commissioning phase and on a somewhat more limited basis during normal operations.

One of the early steps will be to develop an early-adopters program to introduce TEMPO products to potential users. Early-adopters are users who have defined applications for future TEMPO data. Their activities pre-launch will help to identify additional user requirements and applications and thus aid in the exploitation of TEMPO data post-launch.

Air quality and health TEMPO is targeted at improving monitoring, assessment, and chemical understanding of air quality over the United States, Canada, and Mexico. The Decadal Survey emphasized the limitations of the current surface measurement network for air quality applications (NRC 2007). Current observation of air quality from space has been limited so far by the sparseness of LEO satellite data and low sensitivity to near-surface ozone. TEMPO's hourly measurements allow better understanding of the complex chemistry and dynamics that drive air quality on short timescales. The density of TEMPO data is ideally suited for data assimilation into chemical models for both air quality forecasting and for better constraints on emissions that lead to air quality exceedances. Planning is underway to combine TEMPO with regional air quality models to improve EPA air quality indices and to directly supply the public with near real time pollution reports and forecasts through website and mobile applications. The dense spatial coverage of TEMPO will also offer valuable information for epidemiological studies to understand health effects.

As a case study, an OSSE for the Intermountain West was performed to explore the potential of geostationary ozone measurements from TEMPO to improve monitoring of ozone exceedances and the role of background ozone in causing these exceedances [129]. Surface observations are too sparse to adequately monitor high-ozone events in the Intermountain West even when combined with a chemical model. TEMPO geostationary observations will provide a greatly improved observing system for monitoring such events. Fig. 9 shows the ability of TEMPO observations combined with a chemical transport model (GEOS-Chem) to capture the magnitude and spatial structure of a stratospheric intrusion that caused an air quality exceedance. Also, the high spatial resolution of TEMPO will greatly aid in distinguishing and observing over land-sea interfaces. This ability to observe and attribute air pollution events over the entire TEMPO field of regard has great policy and societal benefits. There is existing communication with air quality managers through programs such as the Air Quality Applied Sciences Team (AQAST) that will assist in exploitation of TEMPO data for air quality applications.

Morning and evening higher-frequency scans The optimized data collection scan pattern during mornings and evenings provides multiple advantages for addressing TEMPO science questions. The increased frequency of scans coincides with peaks in vehicle miles traveled on each coast, and thus is better able to capture the variability in NO_x and VOC emissions from mobile sources through measurements of NO_2 and H_2CO. The morning and evening are also of interest for better quantifying the diurnal changes in photochemistry as there is rapid change in the number of available photons. More frequent observations of the morning atmosphere in the Eastern US are of particular benefit since there is usually a rapid rise in ozone concentrations during that time period. Morning NO_x and VOCs are often the primary drivers of peak ozone levels later in the day. More frequent observations lead not only to more accurate quantification of the early morning production of these ozone precursors but also to better assessment and forecasting of peak ozone air quality levels.

Lightning NO_x Lightning-produced NO is the major NO_x source in the upper troposphere and can lead to substantial tropospheric O_3 production there [77]. Interpretation of satellite measurements of tropospheric NO_2 and O_3, and upper tropospheric HNO_3 lead to an overall estimate of $6 \pm 2 \mathrm{Tg\,N\,y^{-1}}$ from lightning [73]. TEMPO measurements, including tropospheric NO_2 and O_3, can be made for time periods and longitudinal bands selected to coincide with large thunderstorm activity, including outflow regions, with fairly short notice. Doing so may be able to significantly better quantify lightning NO_x and O_3 production over greater North America.

Soil NO_x Jaeglé et al. [43] have performed top-down (satellite) partitioning among NO_x sources, including fuel combustion (fossil fuel and biofuel), biomass burning and soils. These are combined with bottom-up inventories to provide much improved a posteriori inventories of NO_x sources and their relative importance. Globally, they estimate $2.5-4.5\ \mathrm{TgN\,y^{-1}}$ are emitted from nitrogen-fertilized soils, still highly uncertain. The U.S. a posteriori estimate for 2000 is $0.86 \pm 1.7\ \mathrm{TgN\,y^{-1}}$. For Central America it is $1.5 \pm 1.6\ \mathrm{TgN\,y^{-1}}$. They note an underestimate of NO release by nitrogen-fertilized croplands as well as an underestimate of rain-induced emissions from semiarid soils.

TEMPO measures greater North America croplands hourly and so is able to follow the temporal evolution of emissions from croplands after fertilizer application and

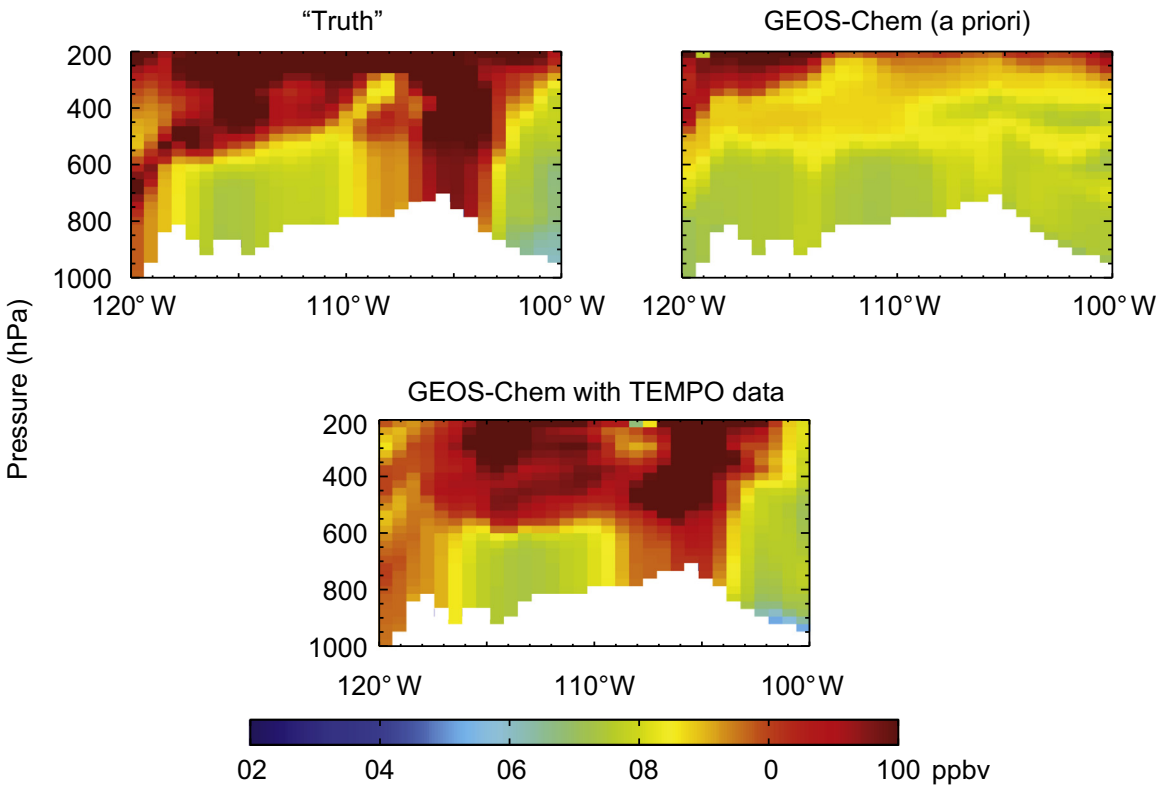

Fig. 9. Longitude-altitude cross-section of ozone concentrations (36°N, 3 GMT on June 14, 2010) associated with a stratospheric intrusion. The "true" state from an independent chemical transport model (top left) is compared to the GEOS-Chem model without data assimilation (top right) and with assimilation of TEMPO data (bottom). Local topography is shown in white. Modified from [129].

from rain-induced emissions from semi-arid soils. Should even higher temporal resolution over selected regions be useful, that may be accomplished by special observations. It has also been noted by Martin et al. [73] that improved constraints on soil NO_x emissions may also improve estimates of lightning NO_x emissions.

Biomass burning Emissions from biomass burning can vary greatly both regionally and from event to event, but previous work has been unable to fully explain this variability. Of particular interest is the unexplained variability in ozone production from fires. The primary emissions from burning and the chemistry in fire plumes evolve on hourly and daily timescales, making observations from TEMPO especially valuable for investigating these processes. The suite of NO_2, H_2CO, $C_2H_2O_2$, O_3, and aerosol measurements from TEMPO is well suited to investigating how the chemical processing of primary fire emissions effects the secondary formation of VOCs and ozone. Ongoing efforts are working to address complications for trace gas retrievals in forest fires due to high aerosol loading [64]. TEMPO measurements should not only increase understanding of the chemical emissions from biomass burning but also be a powerful tool for monitoring and assessing the impact of burning on human health and climate change. For particularly important fires it is possible to command special TEMPO observations at even shorter than hourly revisit time, probably as short as 10 min.

Halogen oxide studies in coastal and lake regions The atmospheric chemistry of halogen oxides (e.g. BrO and IO) over the ocean, and in particular in coastal regions, can play important roles in ozone destruction, oxidizing capacity, and dimethylsulfide oxidation to form cloud-condensation nuclei [91]. The budgets and distribution of reactive halogens along the coastal areas of North America are poorly known. Therefore, providing a measure of the budgets and diurnal evolution of coastal halogen oxides is necessary to understand their role in atmospheric photochemistry of coastal regions. Previous ground-based observations have shown enhanced levels (at a few pptv) of halogen oxides over coastal locations with respect to their background concentrations over the remote marine boundary layer [93]. Previous global satellite instruments lacked the sensitivity and spatial resolution to detect the presence of active halogen chemistry over mid-latitude coastal areas. TEMPO observations together with atmospheric models will allow examination of the processes linking ocean halogen emissions and their potential impact on the oxidizing capacity of coastal environments of North America.

TEMPO also performs hourly measurements of one of the world's largest salt lakes: the Great Salt Lake in Utah. Measurements over Salt Lake City show the highest concentrations of BrO over the globe. Hourly measurement at a high spatial resolution can improve understanding of BrO production in salt lakes.

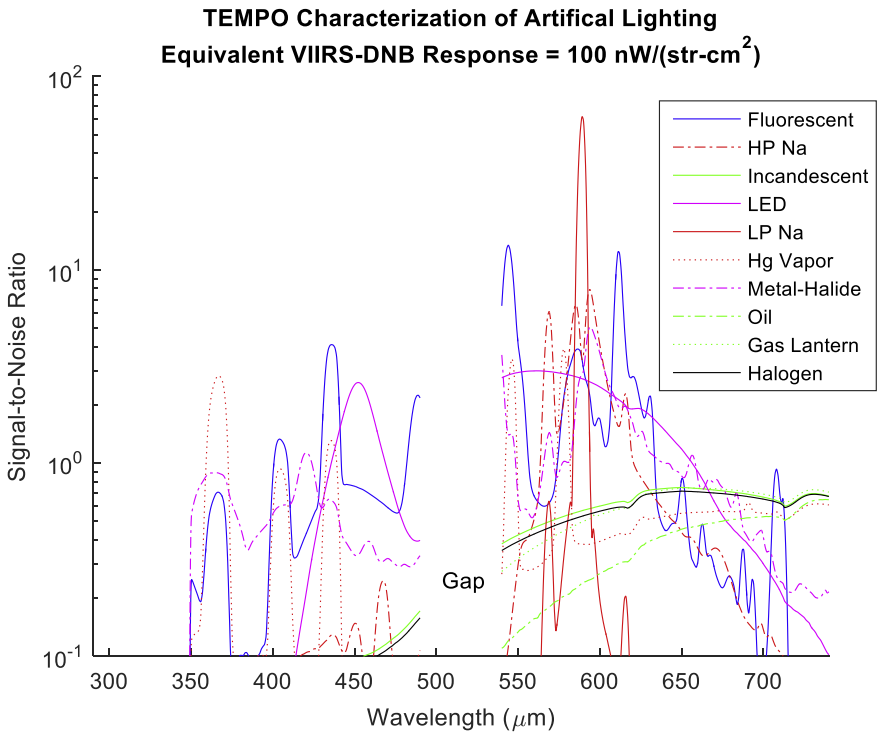

Fig. 10. SNRs of various artificial lighting types normalized to a common VIIRS-DNB response with a 10 s dwell, no co-addition, and no spatial binning, assuming a dark current of 2800 e^- s^{-1}. City lights over all of greater North America can either be observed piecemeal over several days or in a single scan near the winter solstice.

Night lights TEMPO offers the possibility of collecting spectra of nighttime lights when the sun is $>60°$ from its boresight or when the sun is fully eclipsed by the Earth, but direct sunlight cannot be allowed to enter the aperture to possibly damage the spectrometer slit. Because detector well over-filling is less of a concern when collecting over the dark disk, we can reduce the number of co-adds to minimize read-out noise, while also increasing total dwell time, to optimize for nighttime collections. Shot noise from the dark current will be the dominant noise source. Fig. 10 shows the Signal-to-Noise Ratio (SNR) calculated using a TEMPO radiometric model. We use spectra of sources of artificial lighting from the NOAA National Geophysical Data Center [26] and scale their radiances so as to produce an equivalent response in the VIIRS Day-Night Band (DNB) of 100 $nWsr^{-1}$ cm^{-2}, which is an atypically low radiance over an urban area. Incandescent and halogen lighting and combustion sources, which radiate more power at longer wavelengths that are covered by the VIIRS-DNB but not TEMPO, have spectra with low SNR; however, most outdoor lighting in the U.S. is of the High Intensity Discharge (HID) variety [107], such as Hg vapor and high and low pressure Na lamps, which should be detectable by virtue of their narrow spectral features. With 10 s dwell time, TEMPO can map such lights with adequate SNR over greater North America in a single scan of $\sim$3 h near the winter solstice; the domain can be covered piecemeal in several days during other time periods. Weaker signals within a small region can be detected with even longer dwell time. Matched filters tuned to known source spectra will also improve detectability at smaller signal levels. While not specifically intended for nighttime collections, TEMPO provides an interesting capability for studying nightlights as markers for surface aerosol pollution [117], human activity, energy conservation, and compliance with outdoor lighting standards intended to reduce light pollution as described by Elvidge et al. [27].

10. Sharing the TEMPO story: communications, public engagement, and student collaborations

The high spatial resolution and frequently updated datasets of TEMPO – along with the inherent public interest in air quality - provide unique opportunities to engage learners of all ages in the instrument's efforts to track local, regional, and continental trends in air pollution. TEMPO includes a program of Communications and Public Engagement (C/PE) activities led by the Smithsonian Astrophysical Observatory, and a synergistic effort at Langley Research Center that involves students from Minority Serving Institutions in pursuing TEMPO-related air quality research. Together, the TEMPO Student Collaboration and Public Engagement activities aim to achieve the following goals:

- Enhance interest in and public awareness of NASA's efforts to measure the distribution and temporal variation of air pollution across North America, and,

specifically, the story of the TEMPO mission and its components (instrument, technology, team).
- Promote science literacy by using the TEMPO story to communicate the links between basic chemistry, physics, and geoscience concepts, and issues of human health and well-being.
- Empower students, citizen scientists and science communication professionals - including formal and informal educators - in using TEMPO data products to support authentic science engagement.
- Engage a diverse network of students and universities in contributing to TEMPO experimental validation and NASA air quality research.

The activities planned to accomplish these goals include a public-oriented TEMPO website at tempo.si.edu; news and social media activities; the development of a mobile app and user-friendly TEMPO data interfaces (including the EPA's RSIG) to enable citizen science; collaborations with STEM education partners such as the Smithsonian Institution, the GLOBE project and My NASA DATA; public engagement events and programs at museums anchored by a network of Ozone Gardens; and summer internships and research experiences for students and educators at NASA Langley Research Center.

In 2016, the Student Collaboration team at Langley, the SAO Public Engagement team, and the Virginia Living Museum (VLM) are working together to develop and pilot a TEMPO-focused ozone bio-indicator garden, related public outreach materials, and tools and protocols for engaging students and museum visitors in conducting air quality research in the garden. Past Student Collaboration efforts at VLM have included the early development of enhanced protocols for quantifying ozone-induced injury stippling of plants, and time-series measurement of ambient ozone concentrations using small sensors. This work is intended to develop a model for an emerging network of museum-based public ozone gardens that SAO will help to support as TEMPO approaches launch. This work, informed also by the St. Louis Ozone Gardens [30], is intended to develop a model for an emerging network of museum-based public ozone gardens that SAO will help to support as TEMPO approaches launch. The TEMPO Ozone Garden Network will serve as a catalyst for sustained public and citizen science engagement in air quality research during and beyond the TEMPO mission.

11. Summary

The Tropospheric Emissions: Monitoring of Pollution (TEMPO) mission is under development as part of the NASA Earth Venture program to collect the space-based measurements needed to quantify variations in the temporal and spatial emissions of gases and aerosols important for air quality. TEMPO will perform these measurements with the precision, resolution, and coverage needed to improve our understanding of pollutant sources and sinks from sub-urban to regional scales and the processes controlling their variability over the diurnal and seasonal cycles. After the delivery of TEMPO to NASA in 2017, NASA plans to acquire services from a commercial geostationary satellite vendor to operate TEMPO in space.

TEMPO data products include atmospheric ozone profiles, total column ozone, NO_2, SO_2, H_2CO, $C_2H_2O_2$, H_2O, BrO, IO, and aerosol properties, cloud fraction, and cloud top pressure over greater North America. Similar data products are planned across Europe (Sentinel-4), and Asia (GEMS) and, combined with low-elevation orbit (Sentinel-5/5P) observations, can provide full global context. International collaborations enable broader data validation and exploratory product generation. TEMPO's ability to observe and attribute air pollution events over the entire TEMPO field of regard has great policy and societal benefits. TEMPO's time-resolved observations form a truly revolutionary data set for air quality.

Disclaimer

Ball has only approved the section of the paper containing contributions by Dennis Nicks. Accordingly, SAO has agreed to assume sole responsibility for meeting all legal requirements (e.g., contractual, intellectual property, export compliance, customer approval, security requirements, etc.) applicable to the rest of the publication, and Ball Aerospace is absolved of all such responsibilities.

Acknowledgments

The TEMPO Science Team, Instrument Project, Mission Project and Ball Aerospace & Technologies Corp. gratefully acknowledge NASA and their Earth System Science Pathfinder Program for the selection of TEMPO as the first Earth Venture mission and the ongoing support to make it successful. The TEMPO Instrument Project thanks the TEMPO Standing Review Board for tremendous effort that has been central to TEMPO progress. It is always a pleasure to acknowledge the European Space Agency and the German Aerospace Center for support in providing satellite measurements that have been an invaluable asset to TEMPO.

References

[1] Acarreta JR, De Haan JF, Stammes P. Cloud pressure retrieval using the O_2–O_2 absorption band at 477 nm. J Geophys Res 2004;109:2156–202.
[2] Anderson LG, Lanning JA, Barrell R, Miyagishima J, Jones RH, Wolfe P. Sources and sinks of formaldehyde and acetaldehyde: an analysis of Denver's ambient concentration data. Atmos Environ 1996;30:2113–23.
[3] Arellano J, Krüger A, Rivera C, Stremme W, Friedrich MM, Bezanilla A, Grutter M. The MAX-DOAS network in Mexico City to measure atmospheric pollutants. Atmosfera 2016;29(2):157–67.
[4] Arola A, Kazadzis S, Lindfors A, Krotkov N, Kujanpaa J, Tamminen J, et al. A new approach to correct for absorbing aerosols in OMI UV. Geophys Res Lett 2009;36:1944–2007.
[5] Bak J, Liu X, Wei JC, Pan LL, Chance K, Kim JH. Improvement of OMI ozone profile retrievals in the upper troposphere and lower stratosphere by the use of a tropopause-based ozone profile climatology. Atmos Meas Tech 2013;6:2239–54.
[6] Barkley MP, Palmer PI, Kuhn U, Kesselmeier J, Chance K, Kurosu TP, et al. Net ecosystem fluxes of isoprene over tropical South America

inferred from Global Ozone Monitoring Experiment (GOME) observations of HCHO columns. J Geophys Res 2008;113:2156–202.
[7] Boersma KF, Eskes HJ, Dirksen RJ, van d A, Veefkind JP, Stammes P, et al. An improved tropospheric NO_2 column retrieval algorithm for the Ozone Monitoring Instrument. Atmos Meas Tech 2011;4:1905–28.
[8] Brion J, Chakir A, Charbonnier J, Daumont D, Parisse C, Malicet J. Absorption spectra measurements for the ozone molecule in the 350-830 nm region. J. Atmos. Chem. 1998;30:291–9.
[9] Brune WH, Tan D, Faloona IF, Jaegle L, Jacob DJ, Heikes BG, et al. OH and HO 2 chemistry in the North Atlantic free troposphere. Geophys Res Lett 1999;26:3077–80.
[10] Bucsela EJ, Krotkov NA, Celarier EA, Lamsal LN, Swartz WH, Bhartia PK, et al. A new stratospheric and tropospheric NO_2 retrieval algorithm for nadir-viewing satellite instruments: applications to OMI. Atmos Meas Tech 2013;6:2607–26.
[11] Byun D, Schere KL. Review of the governing equations, computational algorithms, and other components of the models-3 Community Multiscale Air Quality (CMAQ) modeling system. Appl Mech Rev 2006;59:51.
[12] Cai Z, Liu Y, Liu X, Chance K, Nowlan CR, Lang R, et al. Characterization and correction of Global Ozone Monitoring Experiment 2 ultraviolet measurements and application to ozone profile retrievals. J Geophys Res: Atmos 2012;117:2156–202.
[13] Carr J. Image Navigation and Registration (INR) transfer from exquisite systems to hosted space payloads. US 14/610,091, January 30, 2015.
[14] CEOS: A geostationary satellite constellation for observing global air quality: an international path forward, 2011.
[15] Chan Miller C, Jacob DJ, Gonzalez Abad G, Chance K. Hotspot of Glyoxal over the Pearl River Delta Seen from the OMI satellite instrument: implications for emissions of aromatic hydrocarbons. Atmos Chem Phys Dis 2016:1–16.
[16] Chance KV, Burrows JP, Perner D, Schneider W. Satellite measurements of atmospheric ozone profiles, including tropospheric ozone, from ultraviolet/visible measurements in the nadir geometry: a potential method to retrieve tropospheric ozone. J Quant Spectrosc Radiat Transfer 1997;57:467–76.
[17] Chance K. Analysis of BrO measurements from the Global Ozone Monitoring Experiment. Geophys Res Lett 1998;25:3335–8.
[18] Chance KV, Burrows JP, Schneider W. Retrieval and molecule sensitivity studies for the global ozone monitoring experiment and the scanning imaging absorption spectrometer for atmospheric chartography. Proc SPIE, Remote Sens Atmos Chem 1991;1491:151–65.
[19] Chance K, Palmer PI, Spurr RJD, Martin RV, Kurosu TP, Jacob DJ. Satellite observations of formaldehyde over North America from GOME. Geophys Res Lett 2000;27:3461–4.
[20] Choi S, Wang Y, Salawitch RJ, Canty T, Joiner J, Zeng T, et al. Analysis of satellite-derived Arctic tropospheric BrO columns in conjunction with aircraft measurements during ARCTAS and ARCPAC. Atmos Chem Phys 2012;12:1255–85.
[21] De Smedt I, Muller JF, Stavrakou T, van d A, Eskes H, Van Roozendael M. Twelve years of global observations of formaldehyde in the troposphere using GOME and SCIAMACHY sensors. Atmos Chem Phys 2008;8:4947–63.
[22] De Smedt I, Van Roozendael M, Stavrakou T, Muller JF, Lerot C, Theys N, et al. Improved retrieval of global tropospheric formaldehyde columns from GOME-2/MetOp-A addressing noise reduction and instrumental degradation issues. Atmos Meas Tech 2012;5:2933–49.
[23] Dirksen RJ, Boersma KF, Eskes HJ, Ionov DV, Bucsela EJ, Levelt PF, et al. Evaluation of stratospheric NO_2 retrieved from the Ozone monitoring Instrument: intercomparison, diurnal cycle, and trending. J Geophys Res 2011;116:D08305.
[24] Dittman MG, Ramberg E, Chrisp M, Rodriguez JV, Sparks AL, Zaun NH, et al. Nadir ultraviolet imaging spectrometer for the NPOESS Ozone Mapping and Profiler Suite (OMPS). Earth Observing Systems VII 2002.
[25] Eck TF, Bhartia PK, Kerr JB. Satellite estimation of spectral UVB irradiance using TOMS derived total ozone and UV reflectivity. Geophys Res Lett 1995;22:611–4.
[26] Laboratory Spectra of Lighting Types: ⟨http://www.ngdc.noaa.gov/eog/night_sat/spectra.html⟩ [accessed 15.01.016].
[27] Elvidge CD, Cinzano P, Pettit DR, Arvesen J, Sutton P, Small C, et al. The Nightsat mission concept. Int J Remote Sens 2007;28:2645–70.
[28] Fioletov VE, McLinden CA, Krotkov N, Li C. Lifetimes and emissions of SO_2 from point sources estimated from OMI. Geophys Res Lett 2015;42:1969–76.
[29] Fioletov VE, McLinden CA, Krotkov N, Yang K, Loyola DG, Valks P, et al. Application of OMI, SCIAMACHY, and GOME-2 satellite SO_2 retrievals for detection of large emission sources. J Geophys Res: Atmos 2013;118(11):399–11,418.
[30] Fishman J, Belina KM, Encarnación CH. The St. Louis ozone gardens: visualizing the impact of a changing atmosphere. Bull Am Meteor Soc 2014;95:1171–6.
[31] Gonzalez Abad G, Liu X, Chance K, Wang H, Kurosu TP, Suleiman R. Updated Smithsonian Astrophysical Observatory Ozone Monitoring Instrument (SAO OMI) formaldehyde retrieval. Atmos Meas Tech 2015;8:19–32.
[32] Gonzalez Abad G, Vasilkov A, Seftor C, Liu X, Chance K. Smithsonian Astrophysical Observatory Ozone Mapping and Profiler Suite (SAO OMPS) formaldehyde retrieval. Atmos Meas Tech Discuss 2015;8:9209–40.
[33] Gonzi S, Palmer PI, Barkley MP, De Smedt I, Van Roozendael M. Biomass burning emission estimates inferred from satellite column measurements of HCHO: Sensitivity to co-emitted aerosol and injection height. Geophys Res Lett 2011;38:L14807.
[34] Grell GA, Peckham SE, Schmitz R, McKeen SA, Frost G, Skamarock WC, et al. Fully coupled "online" chemistry within the WRF model. Atmos. Environ. 2005;39:6957–75.
[35] Gulde ST, Kolm MG, Smith DJ, Maurer R, Bazalgette Courrèges-Lacoste G, Sallusti M, et al. Sentinel-4: a geostationary imaging UVN spectrometer for air quality monitoring – status of design, performance and development, in: Proceedings of the international conference on space optics (ICSO), Spain, 7–10 October 2014.
[36] Helmig D, Thompson CR, Evans J, Boylan P, Hueber J, Park JH. Highly elevated atmospheric levels of volatile organic compounds in the Uintah Basin , Utah. Environ Sci Technol 2014;48:4707–15.
[37] Herman J, Evans R, Cede A, Abuhassan N, Petropavlovskikh I, McConville G. Comparison of ozone retrievals from the Pandora spectrometer system and Dobson spectrophotometer in Boulder, Colorado. Atmos Meas Tech 2015;8:3407–18.
[38] Hou W, Wang J, Xu X, Reid JS. An algorithm for hyperspectral remote sensing of aerosols 2. Information content analysis [in preparation].
[39] Hou W, Wang J, Xu X, Reid JS. An algorithm for hyperspectral remote sensing of aerosols: 1. Development of theoretical framework. J Quant Spectrosc Radiat Transfer 2016;178:400–15.
[40] IGACO. The changing atmosphere: an integrated global atmospheric chemistry observation., Integrated Global Atmospheric Chemistry Observation Theme Team. GAW Rep. 2004;159:1282.
[41] INECC: Acciones para el Fortalecimiento de los Sistemas de Monitoreo de Contaminantes Atmosféricos, Instituto Nacional de Ecología y Cambio Climático, Technical report INE/A1-010/2013, 2013.
[42] Ingmann P, Veihelmann B, Langen J, Lamarre D, Stark H, Courreges-Lacoste GB. Requirements for the GMES Atmosphere Service and ESA's implementation concept: Sentinels-4/−5 and −5p. Remote Sens. Environ 2012;120:58–69.
[43] Jaegle L, Steinberger L, Martin RV, Chance K. Global partitioning of NO_x sources using satellite observations: relative roles of fossil fuel combustion, biomass burning and soil emissions. Faraday Discuss 2005;130:407.
[44] Jobson BT, Volkamer RA, Velasco E, Allwine G, Westberg H, Lamb BK, et al. Comparison of aromatic hydrocarbon measurements made by PTR-MS, DOAS and GC-FID during the MCMA 2003 field experiment. Atmos Chem Phys 2010;10:1989–2005.
[45] Joiner J, Bhartia PK. The determination of cloud pressures from rotational Raman scattering in satellite backscatter ultraviolet measurements. J Geophys Res 1995;100:23019.
[46] Joiner J, Guanter L, Lindstrot R, Voigt M, Vasilkov AP, Middleton EM, et al. Global monitoring of terrestrial chlorophyll fluorescence from moderate-spectral-resolution near-infrared satellite measurements: methodology, simulations, and application to GOME-2. Atmos Meas Tech 2013;6:2803–23.
[47] Joiner J, Schoeberl MR, Vasilkov AP, Oreopoulos L, Platnick S, Livesey NJ, et al. Accurate satellite-derived estimates of the tropospheric ozone impact on the global radiation budget. Atmos Chem Phys 2009;9:4447–65.
[48] Joiner J, Vasilkov AP. First results from the OMI rotational Raman scattering cloud pressure algorithm. IEEE Trans Geosci Remote Sens 2006;44:1272–82.
[49] Joiner J, Vasilkov AP, Bhartia PK, Wind G, Platnick S, Menzel WP. Detection of multi-layer and vertically-extended clouds using A-train sensors. Atmos Meas Tech 2010;3:233–47.
[50] Joiner J, Vasilkov AP, Gupta P, Bhartia PK, Veefkind P, Sneep M, et al. Fast simulators for satellite cloud optical centroid pressure

retrievals; evaluation of OMI cloud retrievals. Atmos Meas Tech 2012;5:529–45.
[51] Joiner J, Yoshida Y, Guanter L, Middleton EM. New methods for retrieval of chlorophyll red fluorescence from hyper-spectral satellite instruments: simulations and application to GOME-2 and SCIAMACHY. Atmos Meas Tech Discuss 2016:1–41.
[52] Joiner J, Bhartia PK, Cebula RP, Hilsenrath E, McPeters RD, Park H. Rotational Raman scattering (Ring effect) in satellite backscatter ultraviolet measurements. Appl Opt 1995;34:4513.
[53] Joiner J, Vasilkov A, Flittner DE, Gleason JF, Bhartia PK. Retrieval of cloud pressure and oceanic chlorophyll content using Raman scattering in GOME ultraviolet spectra. J Geophys Res 2004;109: D01109.
[54] Kaiser J, Wolfe GM, Min KE, Brown SS, Miller CC, Jacob DJ, et al. Reassessing the ratio of glyoxal to formaldehyde as an indicator of hydrocarbon precursor speciation. Atmos Chem Phys 2015;15: 7571–83.
[55] Khokhar MF, Frankenberg C, Van Roozendael M, Beirle S, Kuhl S, Richter A, et al. Satellite observations of atmospheric SO_2 from volcanic eruptions during the time-period of 1996–2002. Adv Space Res 2005;36:879–87.
[56] Kim PS, Jacob DJ, Liu X, Warner JX, Yang K, Chance K, et al. Global ozone–CO correlations from OMI and AIRS: constraints on tropospheric ozone sources. Atmos Chem Phys 2013;13:9321–35.
[57] Knyazikhin Y, Schull MA, Stenberg P, Mottus M, Rautiainen M, Yang Y, et al. Hyperspectral remote sensing of foliar nitrogen content. Proc Natl Acad Sci 2012;110:E185–92.
[58] Koelemeijer RBA. A database of spectral surface reflectivity in the range 335–772 nm derived from 5.5 years of GOME observations. J Geophys Res 2003;108:4070.
[59] Krotkov NA, Bhartia PK, Herman JR, Fioletov V, Kerr J. Satellite estimation of spectral surface UV irradiance in the presence of tropospheric aerosols: 1. Cloud-free case. J Geophys Res 1998;103: 8779.
[60] Krotkov NA, Herman JR, Bhartia PK, Fioletov V, Ahmad Z. Satellite estimation of spectral surface UV irradiance: 2. Effects of homogeneous clouds and snow. J Geophys Res: Atmos 2001;106: 11743–59.
[61] Kujanpaa J, Kalakoski N. Operational surface UV radiation product from GOME-2 and AVHRR/3 data. Atmos Meas Tech 2015;8: 4399–414.
[62] Lamsal LN, Krotkov NA, Celarier EA, Swartz WH, Pickering KE, Bucsela EJ, et al. Evaluation of OMI operational standard NO_2 column retrievals using in situ and surface-based NO_2 observations. Atmos Chem Phys 2014;14:11587–609.
[63] Li C, Joiner J, Krotkov N, Bhartia PK. A fast and sensitive new satellite SO_2 retrieval algorithm based on principal component analysis: application to the ozone monitoring instrument. Geophys Res Lett 2013;40:6314–8.
[64] Lin JT, Liu MY, Xin JY, Boersma KF, Spurr R, Martin R, et al. Influence of aerosols and surface reflectance on satellite NO_2 retrieval: seasonal and spatial characteristics and implications for NO_x emission constraints. Atmos Chem Phys 2015;15:11217–41.
[65] Liu X, Bhartia PK, Chance K, Spurr RJD, Kurosu TP. Ozone profile retrievals from the Ozone Monitoring Instrument. Atmos Chem Phys 2010;10:2521–37.
[66] Liu X, Chance K, Sioris CE, Spurr RJD, Kurosu TP, Martin RV, et al. Ozone profile and tropospheric ozone retrievals from the Global Ozone Monitoring Experiment: algorithm description and validation. J Geophys Res 2005;110:D20307.
[67] Liu X, Chance K, Sioris CE, Kurosu TP, Spurr RJD, Martin RV, et al. Correction to "First directly retrieved global distribution of tropospheric column ozone from GOME: Comparison with the GEOS-CHEM model". J Geophys Res 2006;111.
[68] Liu Z, Wang Y, Vrekoussis M, Richter A, Wittrock F, Burrows JP, et al. Exploring the missing source of glyoxal (CHOCHO) over China. Geophys Res Lett 2012;39:L10812.
[69] Marais EA, Jacob DJ, Jimenez JL, Campuzano-Jost P, Day DA, Hu W, et al. Aqueous-phase mechanism for secondary organic aerosol formation from isoprene: application to the Southeast United States and co-benefit of SO_2 emission controls. Atmos Chem Phys Discuss 2015;15:32005–47.
[70] Marais EA, Jacob DJ, Kurosu TP, Chance K, Murphy JG, Reeves C, et al. Isoprene emissions in Africa inferred from OMI observations of formaldehyde columns. Atmos Chem Phys 2012;12:6219–35.
[71] Martin RV, Chance K, Jacob DJ, Kurosu TP, Spurr RJD, Bucsela E, et al. An improved retrieval of tropospheric nitrogen dioxide from GOME. J Geophys Res 2002;107:4437.
[72] Martin RV, Jacob DJ, Chance K, Kurosu TP, Palmer PI, Evans MJ. Global inventory of nitrogen oxide emissions constrained by space-based observations of NO_2 columns. J Geophys Res 2003;108:4537.
[73] Martin RV, Sauvage B, Folkins I, Sioris CE, Boone C, Bernath P, et al. Space-based constraints on the production of nitric oxide by lightning. J Geophys Res 2007;112:D09309.
[74] McLinden CA, Fioletov V, Boersma KF, Kharol SK, Krotkov N, Lamsal L, et al. Improved satellite retrievals of NO_2 and SO_2 over the Canadian oil sands and comparisons with surface measurements. Atmos Chem Phys 2014;14:3637–56.
[75] McLinden CA, Olsen SC, Hannegan B, Wild O, Prather MJ, Sundet J. Stratospheric ozone in 3-D models: a simple chemistry and the cross-tropopause flux. J Geophys Res 2000;105:14653.
[76] Miles GM, Siddans R, Kerridge BJ, Latter BG, Richards NAD. Tropospheric ozone and ozone profiles retrieved from GOME-2 and their validation. Atmos Meas Tech 2015;8:385–98.
[77] Miyazaki K, Eskes HJ, Sudo K, Zhang C. Global lightning NO_x production estimated by an assimilation of multiple satellite data sets. Atmos Chem Phys 2014;14:3277–305.
[78] National Research Council. Earth science and applications from space: national imperatives for the next decade and beyond. Washington, D.C: National Academy Press; 2007.
[79] Natraj V, Liu X, Kulawik S, Chance K, Chatfield R, Edwards DP, et al. Multi-spectral sensitivity studies for the retrieval of tropospheric and lowermost tropospheric ozone from simulated clear-sky GEO-CAPE measurements. Atmos Environ 2011;45:7151–65.
[80] Nowlan CR, Liu X, Chance K, Cai Z, Kurosu TP, Lee C, et al. Retrievals of sulfur dioxide from the Global Ozone Monitoring Experiment 2 (GOME-2) using an optimal estimation approach: algorithm and initial validation. J Geophys Res 2011;116:D18301.
[81] Nowlan CR, Liu X, Leitch JW, Chance K, Gonzalez Abad G, Liu C, et al. Nitrogen dioxide observations from the Geostationary Trace gas and Aerosol Sensor Optimization (GeoTASO) airborne instrument: retrieval algorithm and measurements during DISCOVER-AQ Texas 2013. Atmos Meas Tech Discuss 2015;8:13099–155.
[82] O'Byrne G, Martin RV, van Donkelaar A, Joiner J, Celarier EA. Surface reflectivity from the Ozone Monitoring Instrument using the Moderate Resolution Imaging Spectroradiometer to eliminate clouds: effects of snow on ultraviolet and visible trace gas retrievals. J Geophys Res 2010;115.
[83] Palmer PI. Mapping isoprene emissions over North America using formaldehyde column observations from space. J Geophys Res 2003;108.
[84] Palmer PI, Jacob DJ, Chance K, Martin RV, Spurr RJD, Kurosu TP, et al. Air mass factor formulation for spectroscopic measurements from satellites: application to formaldehyde retrievals from the Global Ozone Monitoring Experiment. J Geophys Res 2001;106: 14539.
[85] Park SS, Kim J, Lee H, Torres O, Lee KM, Lee SD. Utilization of O_4 slant column density to derive aerosol layer height from a space-borne UV–visible hyperspectral sensor: sensitivity and case study. Atmos Chem Phys Discuss 2015;15:7933–75.
[86] Pierce RB, Schaack T, Al-Saadi J, Fairlie TD, Kittaka C, Lingenfelser G, et al. Chemical data assimilation estimates of continental U.S. ozone and nitrogen budgets during the Intercontinental Chemical Transport Experiment-North America. J Geophys Res 2007;112: D12S21.
[87] Richter A, Burrows JP. Tropospheric NO_2 from GOME measurements. Adv Space Res 2002;29:1673–83.
[88] Richter A, Begoin M, Hilboll A, Burrows JP. An improved NO_2 retrieval for the GOME-2 satellite instrument. Atmos Meas Tech 2011;4:1147–59.
[89] Rodgers CD. Inverse methods for atmospheric sounding. 2000.
[90] Saiz-Lopez A, Chance K, Liu X, Kurosu TP, Sander SP. First observations of iodine oxide from space. Geophys Res Lett 2007;34: L12812.
[91] Saiz-Lopez A, von Glasow R. Reactive halogen chemistry in the troposphere. Chem Soc Rev 2012;41:6448.
[92] Schmit TJ, Gunshor MM, Menzel WP, Gurka JJ, Li J, Bachmeier AS. Introducing the next-generation advanced baseline imager on GOES-R. Bull Am Meteor Soc 2005;86:1079–96.
[93] Simpson WR, Brown SS, Saiz-Lopez A, Thornton JA, Glasow RV. Tropospheric halogen chemistry: sources, cycling, and impacts. Chem Rev 2015;115:4035–62.
[94] Sneep M, de Haan JF, Stammes P, Wang P, Vanbauce C, Joiner J, et al. Three-way comparison between OMI and PARASOL cloud pressure products. J Geophys Res 2008;113:D15S23.
[95] Speed J, Carr J, Gutierrez H, Nicks D. GEO-hosted imaging spectrometer, Proceedings of the 38th annual AAS rocky mountain

guidance and control conference. Advances in the Astronautical Sciences 2016;vol. 155.
[96] Spurr R, Natraj V, Lerot C, Van Roozendael M, Loyola D. Linearization of the Principal Component Analysis method for radiative transfer acceleration: application to retrieval algorithms and sensitivity studies. J Quant Spectrosc Radiat Transfer 2013;125:1–17.
[97] Spurr R. LIDORT and VLIDORT: Linearized pseudo-spherical scalar and vector discrete ordinate radiative transfer models for use in remote sensing retrieval problems. Light Scatter Rev 2008;3:229–75.
[98] Spurr RJD. VLIDORT: A linearized pseudo-spherical vector discrete ordinate radiative transfer code for forward model and retrieval studies in multilayer multiple scattering media. J Quant Spectrosc Radiat Transfer 2006;102:316–42.
[99] Stammes P, Sneep M, de Haan JF, Veefkind JP, Wang P, Levelt PF. Effective cloud fractions from the Ozone Monitoring Instrument: theoretical framework and validation. J Geophys Res 2008;113:D16S38.
[100] Streets DG, Canty T, Carmichael GR, de Foy B, Dickerson RR, Duncan BN, et al. Emissions estimation from satellite retrievals: a review of current capability. Atmos Environ 2013;77:1011–42.
[101] Tanskanen A, Lindfors A, Maatta A, Krotkov N, Herman J, Kaurola J, et al. Validation of daily erythemal doses from Ozone Monitoring Instrument with ground-based UV measurement data. J Geophys Res 2007;112:D24S44.
[102] Thalman R, Volkamer R. Temperature dependent absorption cross-sections of O_2-O_2 collision pairs between 340 and 630 nm and at atmospherically relevant pressure. Phys Chem Chem Phys 2013;15:15371.
[103] Theys N, Van Roozendael M, Hendrick F, Yang X, De Smedt I, Richter A, et al. Global observations of tropospheric BrO columns using GOME-2 satellite data. Atmos Chem Phys 2011;11:1791–811.
[104] Torres O, Ahn C, Chen Z. Improvements to the OMI near UV aerosol algorithm using A-train CALIOP and AIRS observations. Atmos Meas Tech Discuss 2013;6:5621–52.
[105] Torres O, Tanskanen A, Veihelmann B, Ahn C, Braak R, Bhartia PK, et al. Aerosols and surface UV products from Ozone Monitoring Instrument observations: an overview. J Geophys Res 2007;112:D24S47.
[106] Turner AJ, Jacob DJ, Wecht KJ, Maasakkers JD, Lundgren E, Andrews AE, et al. Estimating global and North American methane emissions with high spatial resolution using GOSAT satellite data. Atmos Chem Phys 2015;15:7049–69.
[107] U.S. Department of Energy: 2010 U.S. Lighting Market Characterization, Office of Energy Efficiency and Renewable Energy: 2012.
[108] Ustin SL, Gitelson AA, Jacquemoud S, Schaepman M, Asner GP, Gamon JA, et al. Retrieval of foliar information about plant pigment systems from high resolution spectroscopy. Remote Sens Environ 2009;113:S67–77.
[109] Valin LC, Russell AR, Hudman RC, Cohen RC. Effects of model resolution on the interpretation of satellite NO_2 observations. Atmos Chem Phys 2011;11:11647–55.
[110] Vasilkov A, Joiner J, Seftor C. First results from a rotational Raman scattering cloud algorithm applied to the Suomi National Polar-orbiting Partnership (NPP) Ozone Mapping Profiler Spectrometer (OMPS) nadir mapper. Atmos Meas Tech Discuss 2014;7:2689–714.
[111] Vasilkov A, Joiner J, Yang K, Bhartia PK. Improving total column ozone retrievals by using cloud pressures derived from Raman scattering in the UV. Geophys Res Lett 2004;31:L20109.
[112] Vasilkov A, Joiner J, Spurr R, Bhartia PK, Levelt P, Stephens G. Evaluation of the OMI cloud pressures derived from rotational Raman scattering by comparisons with other satellite data and radiative transfer simulations. J Geophys Res 2008;113:D15S19.
[113] Veihelmann B, Meijer Y, Ingmann P, Koopman R, Wright N, Bazalgette Courrèges-Lacoste G, et al. The Sentinel-4 mission and its atmospheric composition products. In: Proceedings of the 2015 EUMETSAT meteorological satellite conference. France, 21–25 September 2015.
[114] Volkamer R, San Martini F, Molina LT, Salcedo D, Jimenez JL, Molina MJ. A missing sink for gas-phase glyoxal in Mexico City: formation of secondary organic aerosol. Geophys Res Lett 2007;34:L19807.
[115] Wagner T, Beirle S, Sihler HA, Mies K. A feasibility study for the retrieval of the total column precipitable water vapour from satellite observations in the blue spectral range. Atmos Meas Tech 2013;6:2593–605.
[116] Wang H, Liu X, Chance K, Gonzalez Abad G, Chan Miller C. Water vapor retrieval from OMI visible spectra. Atmos Meas Tech 2014;7:1901–13.
[117] Wang H, Gonzalez Abad G, Liu X, Chance K. Validation of OMI total column water vapor product. Atmos Chem Phys Discuss 2016. http://dx.doi.org/10.5194/acp-2016-181.
[118] Wang J, Liu X, Christopher SA, Reid JS, Reid E, Maring H. The effects of non-sphericity on geostationary satellite retrievals of dust aerosols. Geophys Res Lett 2003;30:2293.
[119] Wang J, Xu X, Ding S, Zeng J, Spurr R, Liu X, et al. A numerical testbed for remote sensing of aerosols, and its demonstration for evaluating retrieval synergy from a geostationary satellite constellation of GEO-CAPE and GOES-R. J Quant Spectrosc Radiat Transfer 2014;146:510–28.
[120] Wang J, Aegerter C, Xu X, Szykman JJ. Potential application of VIIRS Day/Night Band for monitoring nighttime surface PM2.5 air quality from space. Atmos Environ 2016;124:55–63. http://dx.doi.org/10.1016/j.atmosenv.2015.11.013.
[121] Washenfelder RA, Young CJ, Brown SS, Angevine WM, Atlas EL, Blake DR, et al. The glyoxal budget and its contribution to organic aerosol for Los Angeles, California, during CalNex 2010. J Geophys Res 2011;116:D00V02.
[122] Wolfe GM, Kaiser J, Hanisco TF, Keutsch FN, de Gouw JA, Gilman JB, et al. Formaldehyde production from isoprene oxidation across NO_x regimes. Atmos Chem Phys Discuss 2015;15:31587–620.
[123] Zhang H, Hoff RM, Kondragunta S, Laszlo I, Lyapustin A. Aerosol optical depth (AOD) retrieval using simultaneous GOES-East and GOES-West reflected radiances over the western United States. Atmos Meas Tech 2013;6:471–86.
[124] Zhang L, Jacob DJ, Liu X, Logan JA, Chance K, Eldering A, et al. Intercomparison methods for satellite measurements of atmospheric composition: application to tropospheric ozone from TES and OMI. Atmos Chem Phys Discusss 2010;10:1417–56.
[125] Zhang L, Jacob DJ, Boersma KF, Jaffe DA, Olson JR, Bowman KW, et al. Transpacific transport of ozone pollution and the effect of recent Asian emission increases on air quality in North America: an integrated analysis using satellite, aircraft, ozonesonde, and surface observations. Atmos Chem Phys 2008;8:6117–36.
[126] Zhu L, Jacob DJ, Chance K, Gonzalez Abad G:. Observing atmospheric formaldehyde (HCHO) from space: validation and intercomparison of six retrievals from four satellites (OMI, GOME2A, GOME2B, OMPS) with SEAC4RS aircraft observations over the Southeast US. Atmos Chem Phys Discuss 2016:1–14.
[127] Zhu L, Jacob DJ, Mickley LJ, Marais EA, Cohan DS, Yoshida Y, et al. Anthropogenic emissions of highly reactive volatile organic compounds in eastern Texas inferred from oversampling of satellite (OMI) measurements of HCHO columns. Environ Res Lett 2014;9:114004.
[128] Zoogman P, Liu X, Chance K, Sun Q, Schaaf C, Mahr T, et al. A climatology of visible surface reflectance spectra. JQSRT 2016;180:39–46.
[129] Zoogman P, Jacob DJ, Chance K, Liu X, Lin M, Fiore A, et al. Monitoring high-ozone events in the US Intermountain West using TEMPO geostationary satellite observations. Atmos Chem Phys 2014;14:6261–71.
[130] Zoogman P, Jacob DJ, Chance K, Zhang L, Le Sager P, Fiore AM, et al. Ozone air quality measurement requirements for a geostationary satellite mission. Atmos Environ 2011;45:7143–50.